

SUPPLEMENT TO UPC 30

We have discussed some of the typical cases in which the proton beam strikes the vacuum chamber of the Doubler magnets on the inside edge. In this supplement we report various cases in which protons strike different parts of the vacuum chamber with various incident angles. The vacuum chamber radius is either from 3.18 cm to 3.31 cm or from 3.68 cm to 3.81 cm. The incident beam angle at which protons strike the vacuum chamber with respect to the perfect beam orbit direction is either ± 0.7 mrad, or zero (parallel incidence). The positive (negative) angle corresponds to a beam moving outward (inward) in the accelerator radius direction. The incident angle of ± 0.7 mrad is roughly the maximum beam divergency angle after defocussing quadrupole magnets in the accelerator. The incident angle of 0 mrad corresponds to parallel beam particles along the vacuum chamber side wall. In the parallel case, when protons hit the edge of the vacuum chamber or plug, the probability that some of the protons are scattered out due to Coulomb scattering before nuclear interaction was crudely taken into account.

Figures S1 through S21 show energy density distributions in the Doubler magnet coils as functions of azimuthal angle and coil radius. Table I summarizes some of the interesting properties for all the cases.

The maximum energy deposition at the upstream end and in the shallow radial region of coils (3.81 cm to 4.4 cm) is very sensitive to the vacuum chamber radius. The maximum energy deposition is reduced by a factor of about 5 by changing the chamber inner radius from 3.68 cm to 3.18 cm in all the cases discussed here. The second peaks due to neutral pion production depend strongly upon beam conditions because the vacuum chamber material can absorb

photons from the neutral pion decay.

The energy deposition in the large radial region of coils (4.4 cm to 5.0 cm) is substantially smaller than that in the shallow region. This is due to shielding by the coil material itself.

The vacuum chamber plug suppresses the energy deposition level to 0.01 GeV/(cm³ interacting proton) or less except for in the upstream end region.

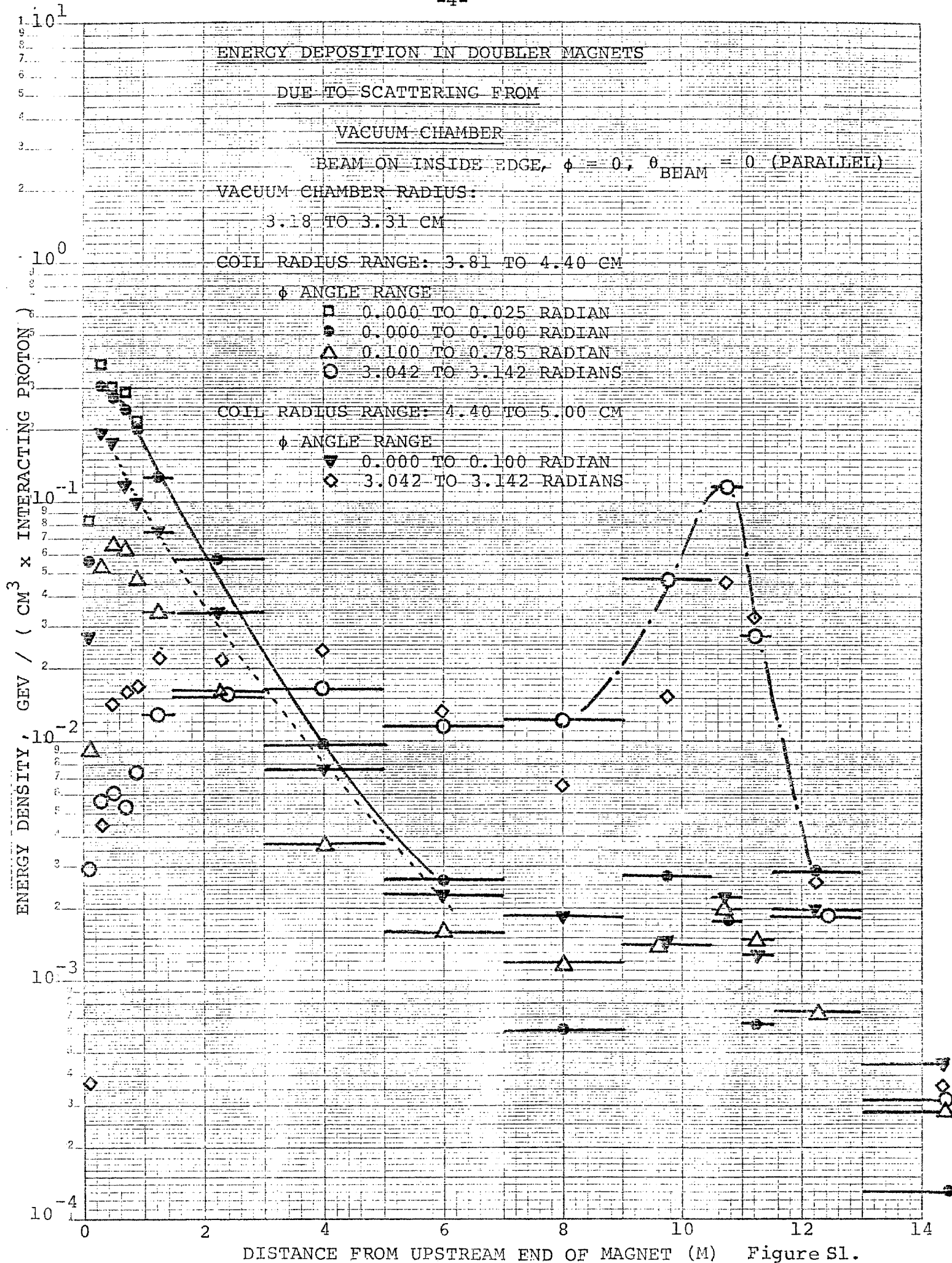
TABLE I

Vacuum Chamber Inner Radius (cm)	Beam Position on Chamber Radius	ϕ (rad)	θ_{Beam} (mrad)	Maximum Energy Deposition, $\text{GeV}/(\text{cm}^3 \cdot \text{Int. Protons})$		
				Coil Radius: 3.81-4.40 cm	Upstream (ϕ)	2nd peak* (ϕ)
S1	3.18	Inside	0	0	0.38 (0)	0.12 (π)
S2	3.18	Inside	0	+0.7	0.56 (0)	0.03 (π)
S3	3.18	Middle	0	0	0.85 (0)	0.003 (π)
S4	3.18	Middle	0	+0.7	0.88 (0)	0.001 (π)
S5	3.18	Outside	0	0	0.67 (0)	0.01 (0)
S6	3.68	Inside	0	0	1.9 (0)	0.12 (π)
S7	3.68	Inside	0	+0.7	2.6 (0)	0.06 (π)
S8	3.68	Middle	0	+0.7	5.4 (0)	0.001 (π)
S9	3.18	Inside	π	0	0.30 (π)	0.015 (0)
S10	3.18	Inside	π	-0.7	0.52 (π)	0.006 (0)
S11	3.18	Middle	π	0	0.82 (π)	0.001 (0)
S12	3.18	Middle	π	-0.7	0.80 (π)	0.001 (π)
S13	3.18	Outside	π	0	0.61 (π)	0.004 (π)
S14	3.68	Inside	π	0	2.2 (π)	0.02 (0)
S15	3.68	Inside	π	-0.7	2.9 (π)	0.006 (0)
S16	3.68	Middle	π	-0.7	5.7 (π)	0.0005 (?)
S17	3.68	Outside	π	-0.7	9.0 (π)	0.0005 (?)
S18	Plug**	Inside	0	0	0.09 (0)	0.01 (π)
S19	Plug	Inside	0	+0.7	0.15 (0)	0.004 (π)
S20	Plug	Inside	π	0	0.10 (π)	0.005 (0)
S21	Plug	Inside	π	-0.7	0.12 (π)	0.002 (0)

-3-

* when no apparent second peak appears, the maximum energy deposition at about 10m from the upstream end of the Doubler magnet is quoted.

** the aperture of the vacuum chamber plug hole is 5cm (horizontal) x 3cm (vertical). The space between the coils and the plug aperture is filled with iron.



ENERGY DEPOSITION IN DOUBLER MAGNETS
DUE TO SCATTERING FROM
VACUUM CHAMBER

BEAM ON INSIDE EDGE

$\phi = 0$, $\theta_{\text{BEAM}} = 0.7 \text{ MRAD}$

VACUUM CHAMBER RADIUS: 3.18 TO 3.31 CM

COIL RADIAL RANGE: 3.81 TO 4.40 CM

ϕ ANGULAR RANGE

\square 0.000 TO 0.025 RADIANS

\bullet 0.000 TO 0.100 RADIANS

Δ 0.100 TO 0.785 RADIANS

\circ 3.042 TO 3.142 RADIANS

COIL RADIAL RANGE: 4.40 TO 5.00 CM

ϕ ANGULAR RANGE

\blacktriangledown 0.000 TO 0.100 RADIANS

\diamond 3.042 TO 3.142 RADIANS

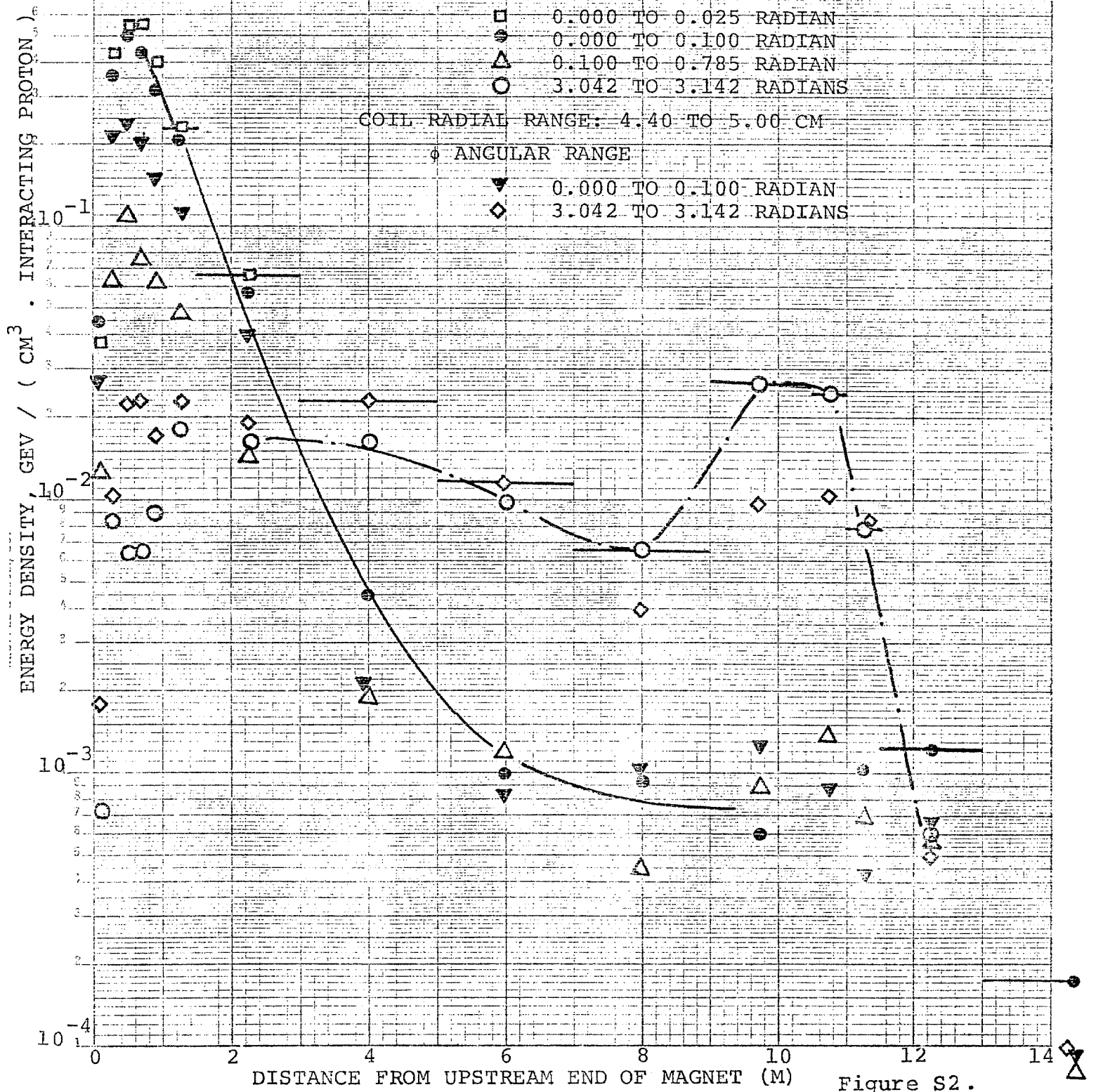


Figure S2.

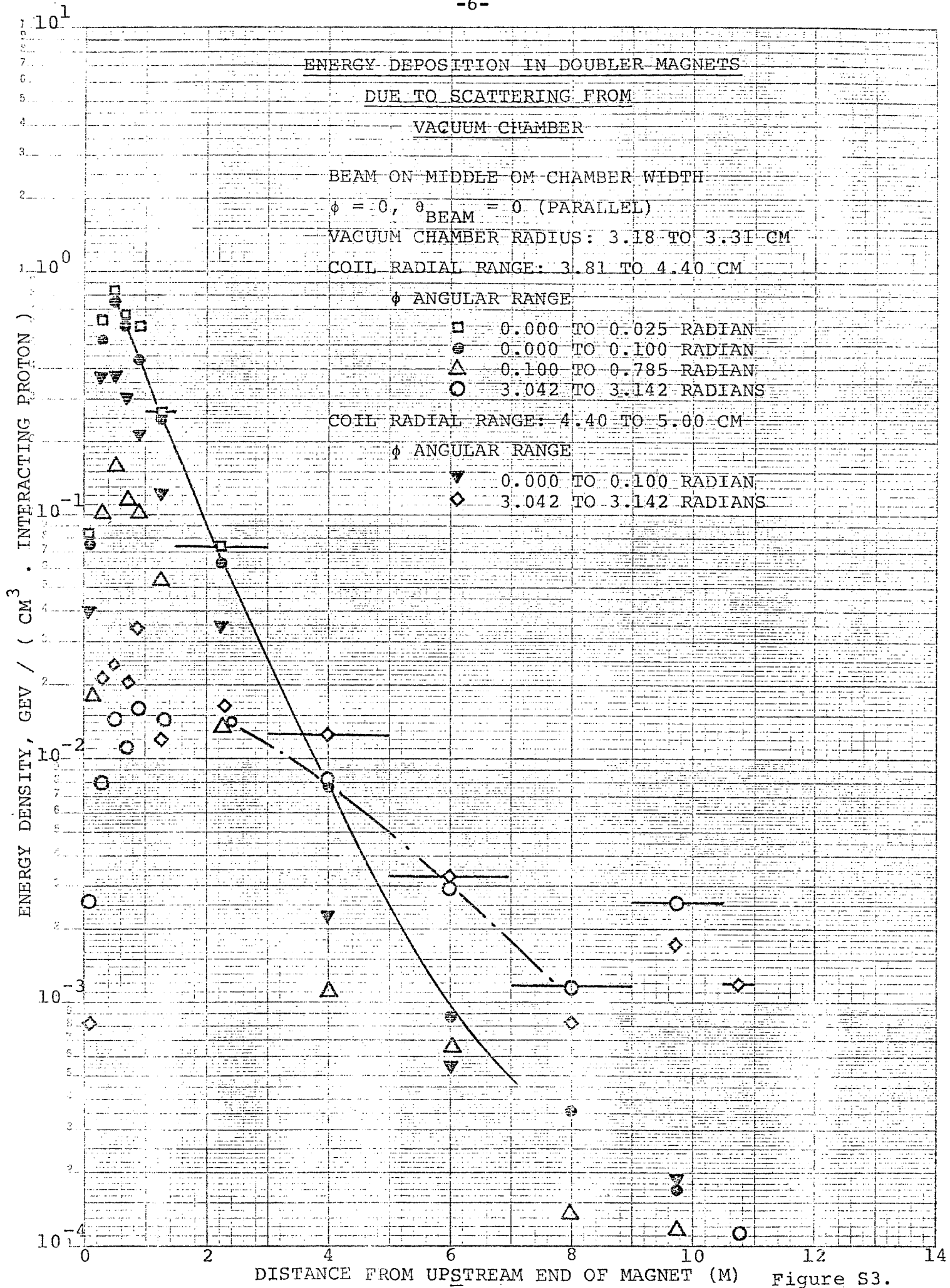


Figure S3.

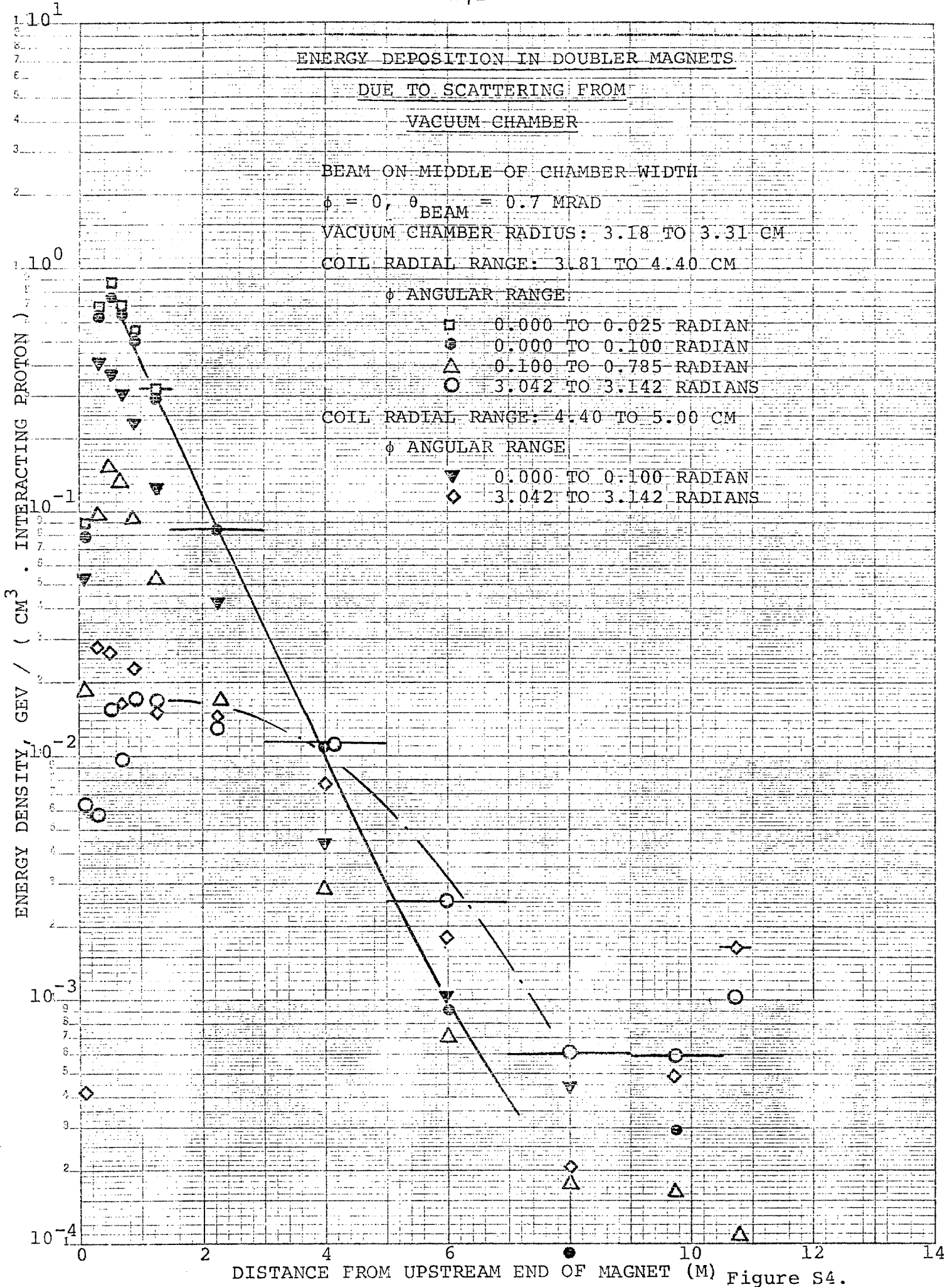


Figure S4.

ENERGY DEPOSITION IN DOUBLER MAGNETS
DUE TO SCATTERING FROM
VACUUM CHAMBER

BEAM ON OUTSIDE EDGE

$\phi = 0, \theta_{\text{BEAM}} = 0$ (PARALLEL)

VACUUM CHAMBER RADIUS: 3.18 TO 3.31 CM

COIL RADIAL RANGE: 3.81 TO 4.40 CM

ϕ ANGULAR RANGE

□ 0.000 TO 0.025 RADIANS

● 0.000 TO 0.100 RADIANS

△ 0.100 TO 0.785 RADIANS

○ 3.042 TO 3.142 RADIANS

COIL RADIAL RANGE: 4.40 TO 5.00 CM

ϕ ANGULAR RANGE

▽ 0.000 TO 0.100 RADIANS

◇ 3.042 TO 3.142 RADIANS

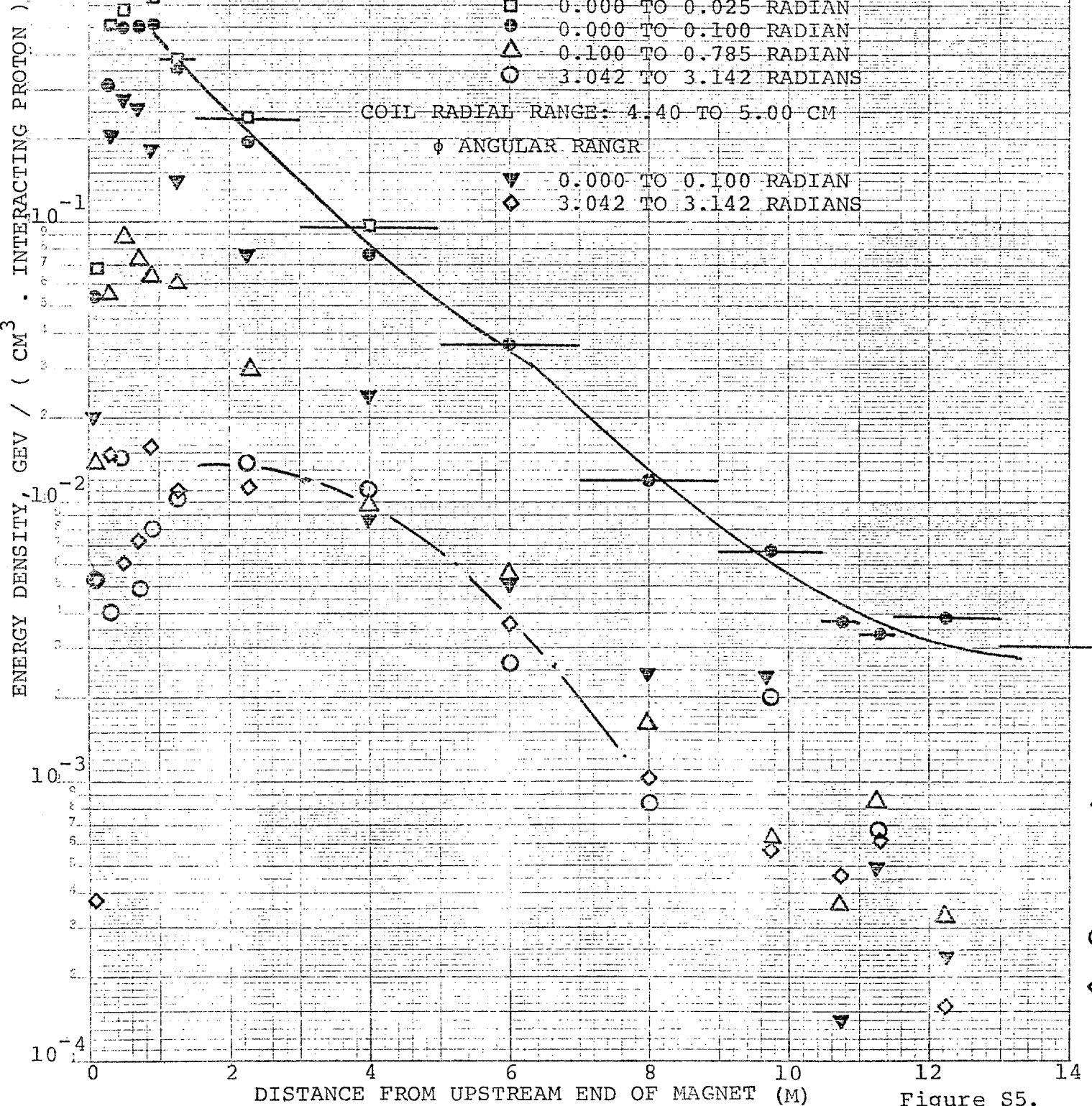


Figure S5.

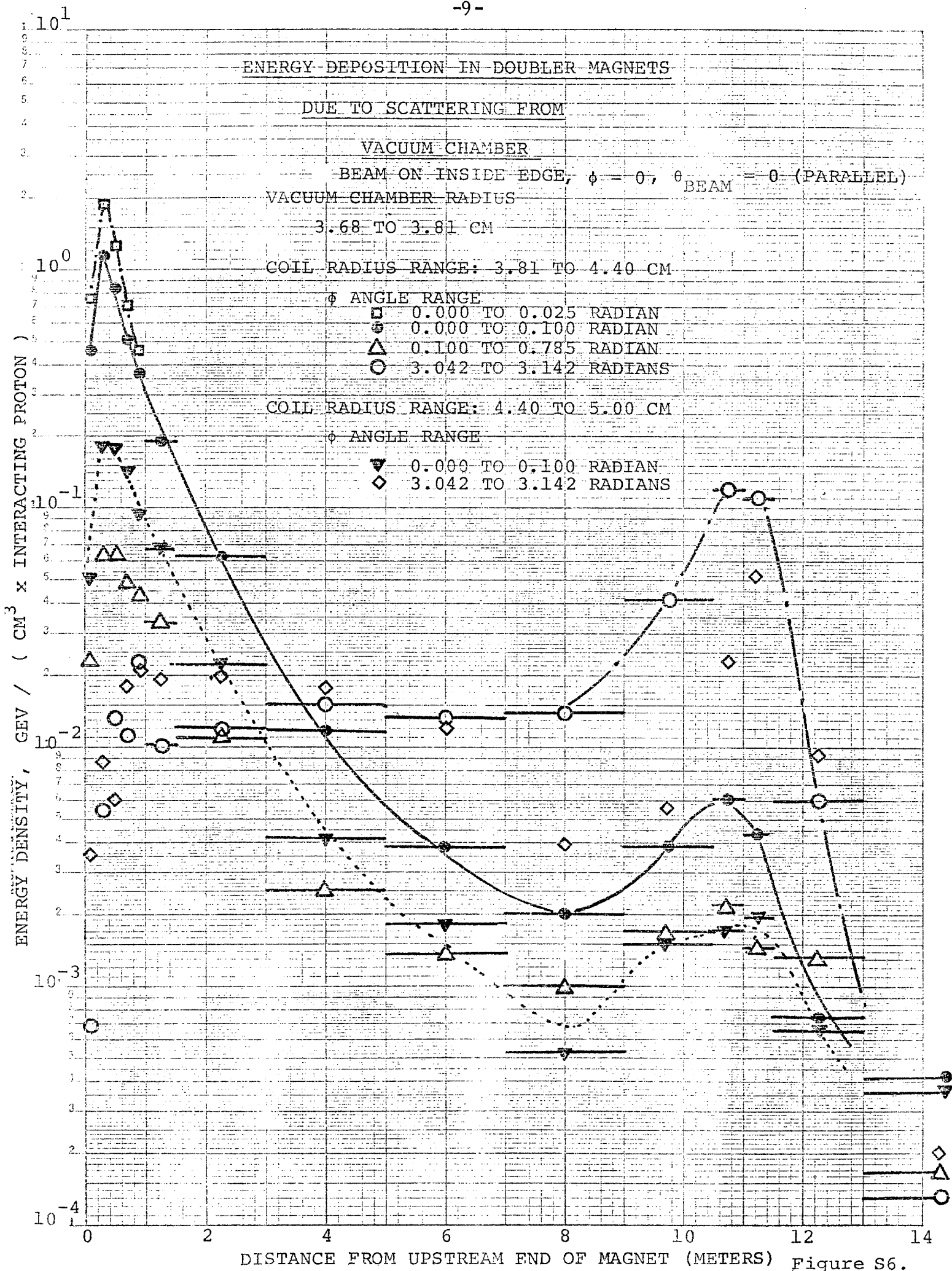


Figure S6.

ENERGY DEPOSITION IN DOUBLER MAGNETS
DUE TO SCATTERING FROM
VACUUM CHAMBER

BEAM ON INSIDE EDGE

$\phi = 0$, BEAM = 0.7 MRAD

VACUUM CHAMBER RADIUS: 3.68 TO 3.81 CM

COIL RADIAL RANGE: 3.81 TO 4.40 CM

ϕ ANGULAR RANGE

□ 0.000 TO 0.025 RADIANS

● 0.000 TO 0.100 RADIANS

△ 0.100 TO 0.735 RADIANS

○ 3.042 TO 3.142 RADIANS

COIL RADIAL RANGE: 4.40 TO 5.00 CM

ϕ ANGULAR RANGE

▽ 0.000 TO 0.100 RADIANS

◇ 3.042 TO 3.142 RADIANS

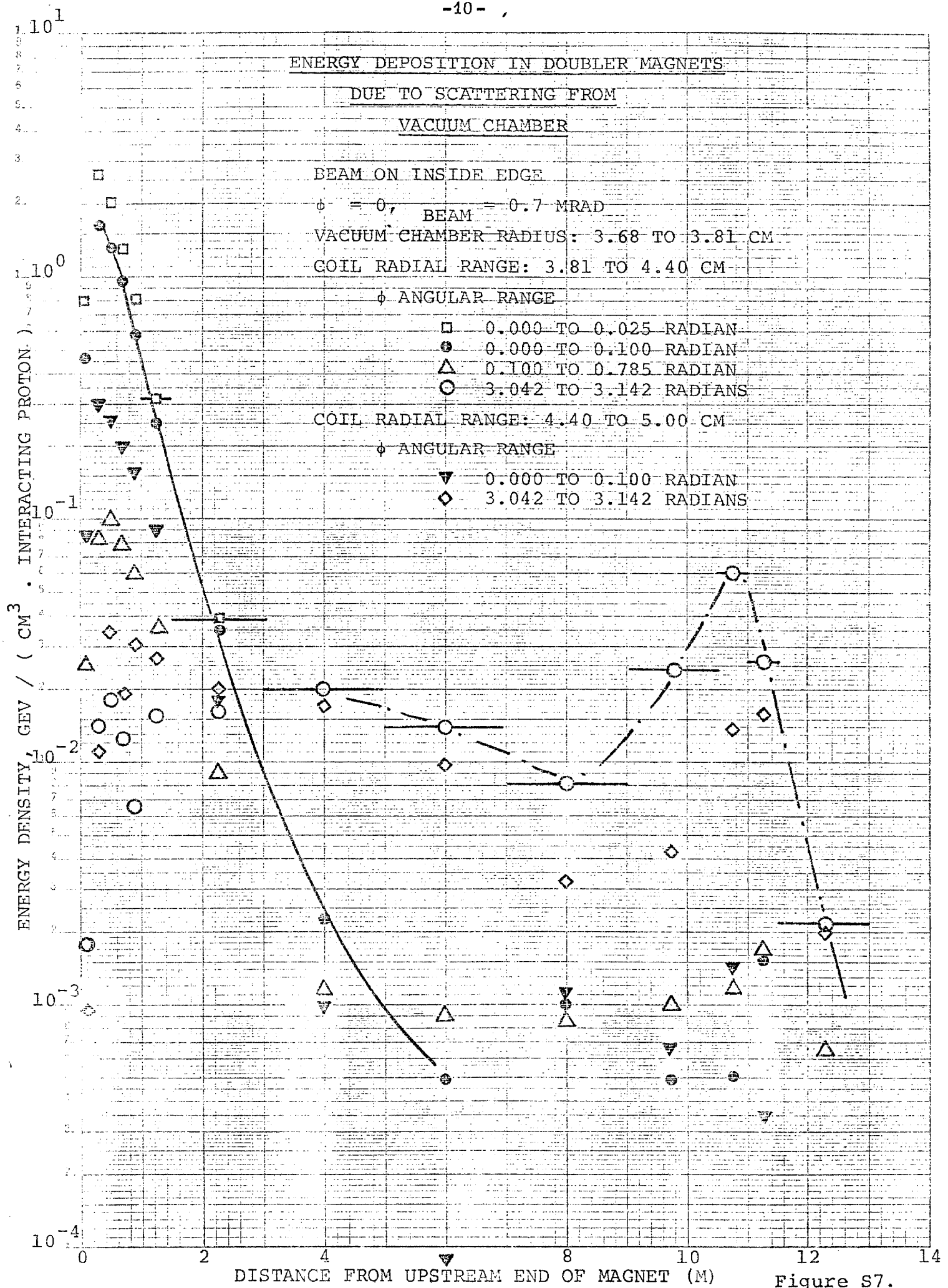


Figure S7.

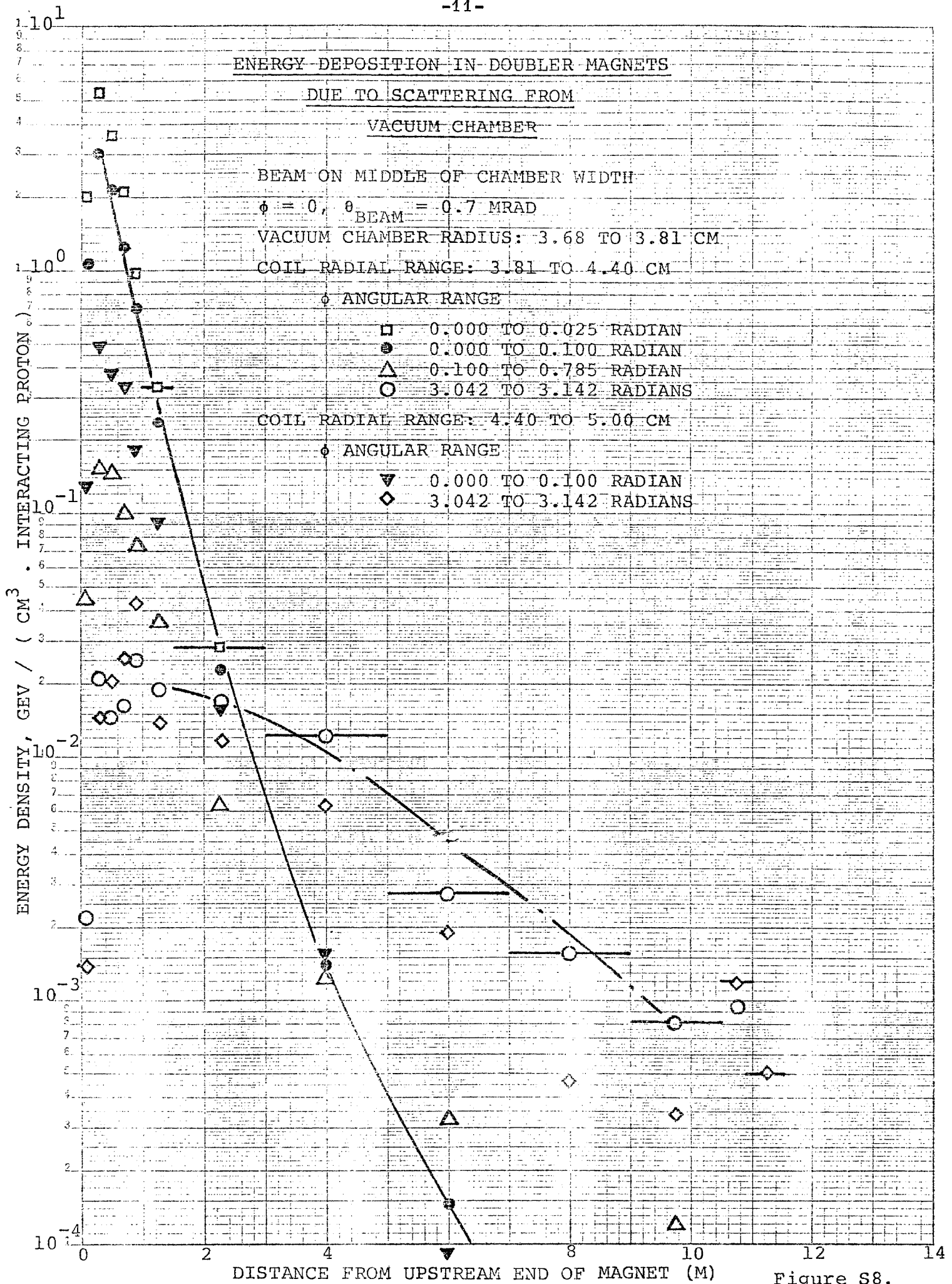
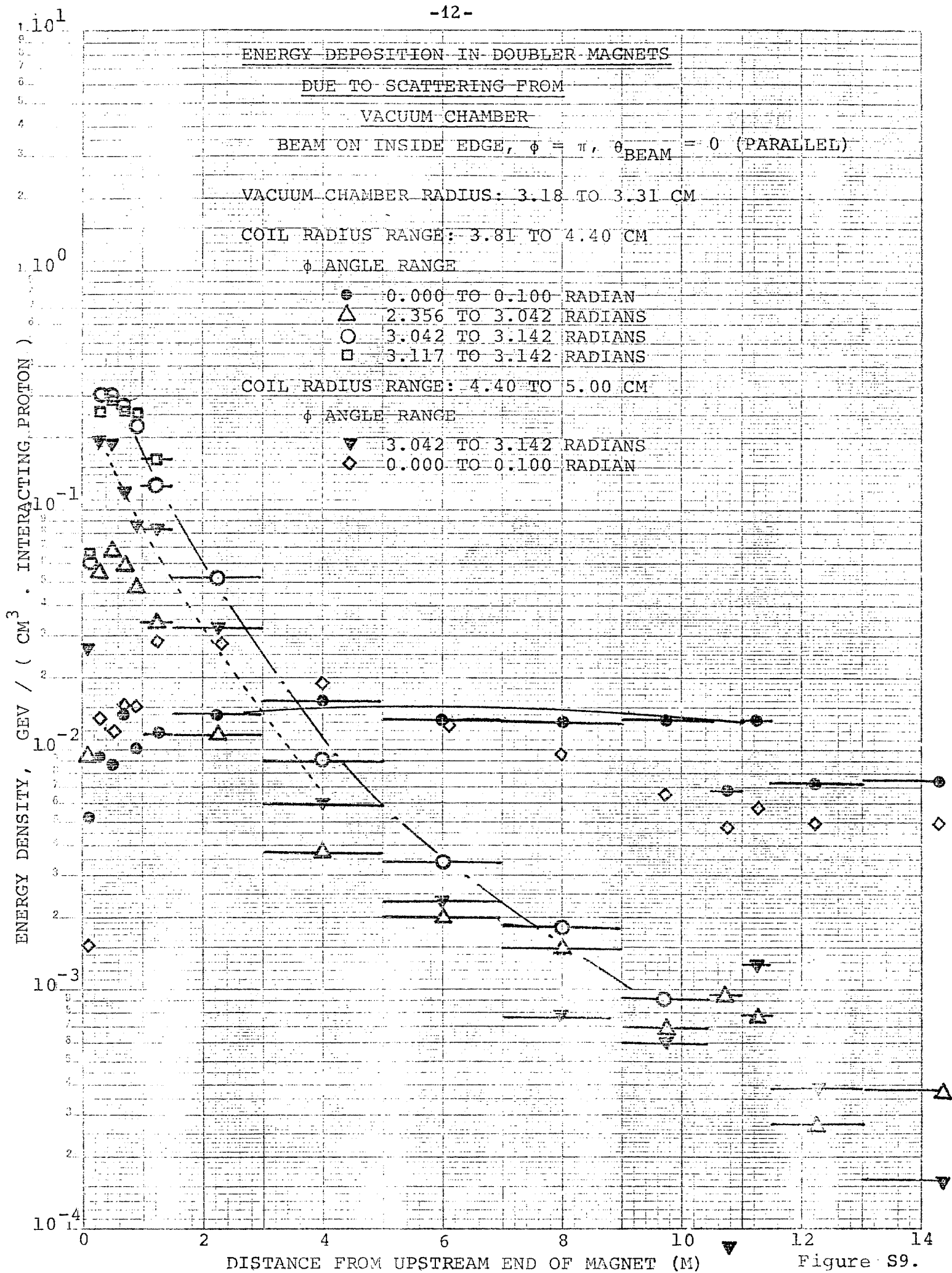


Figure S8.



ENERGY DEPOSITION IN DOUBLER MAGNETS
DUE TO SCATTERING FROM
VACUUM CHAMBER

BEAM ON INSIDE EDGE

$\phi = \pi$, $\theta_{\text{BEAM}} = -0.7$ MRAD

VACUUM CHAMBER RADIUS: 3.18 TO 3.31 CM

COIL RADIAL RANGE: 3.81 TO 4.40 CM

ϕ ANGULAR RANGE

● 0.000 TO 0.100 RADIANS

△ 2.356 TO 3.042 RADIANS

○ 3.042 TO 3.142 RADIANS

□ 3.117 TO 3.142 RADIANS

COIL RADIAL RANGE: 4.40 TO 5.00 CM

ϕ ANGULAR RANGE

▼ 3.042 TO 3.142 RADIANS

◇ 0.000 TO 0.100 RADIANS

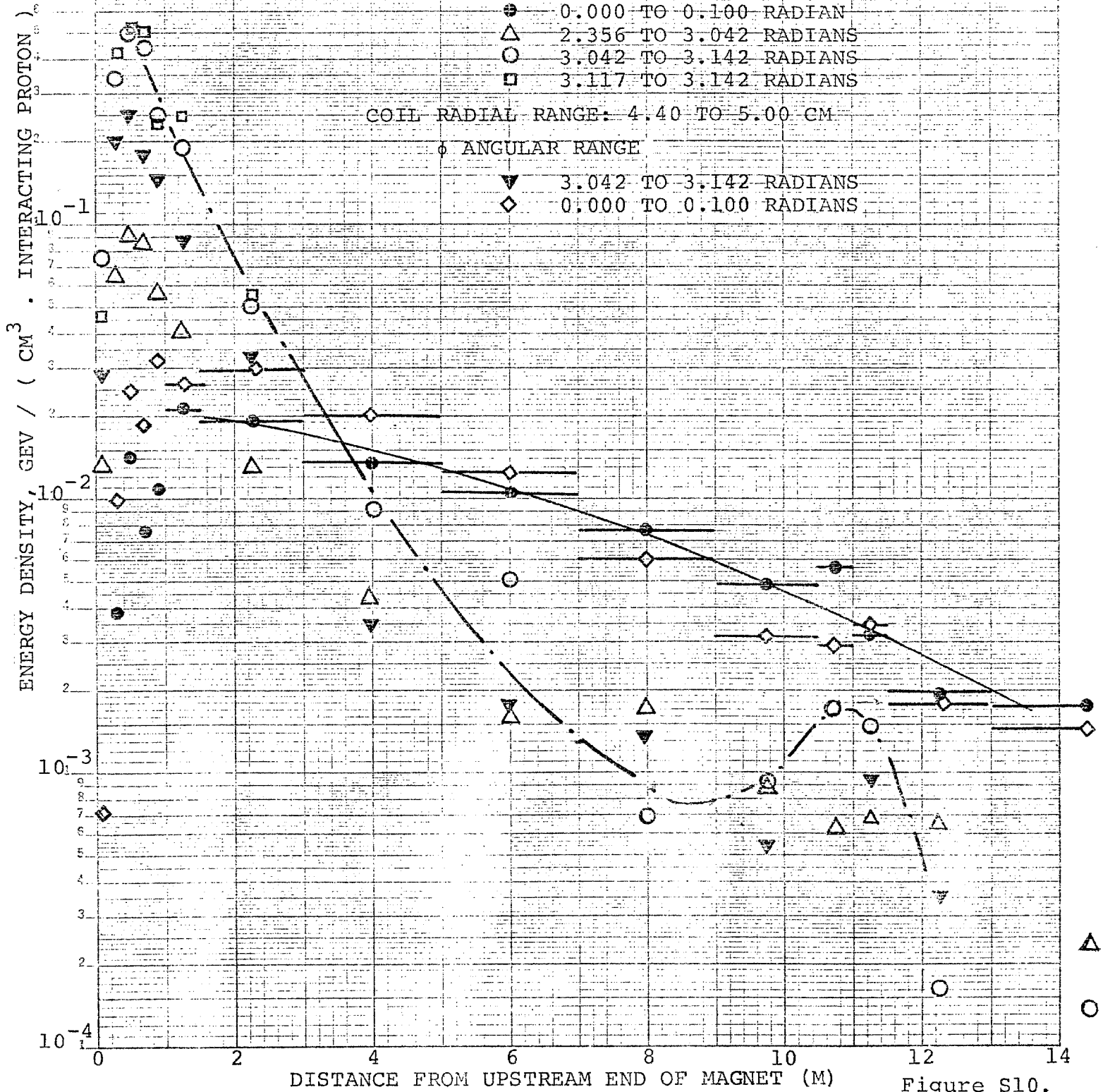


Figure S10.

ENERGY DEPOSITION IN DOUBLER MAGNETS

DUE TO SCATTERING FROM

VACUUM CHAMBER

BEAM ON MIDDLE OF CHAMBER WIDTH

$\phi = \pi$, $\theta = 0$ (PARALLEL)

VACUUM CHAMBER RADIUS: 3.18 TO 3.31 CM

COIL RADIAL RANGE: 3.81 TO 4.40 CM

ϕ ANGULAR RANGE

0.000 TO 0.100 RADIAN

2.356 TO 3.042 RADIAN

3.042 TO 3.142 RADIAN

3.117 TO 3.142 RADIAN

COIL RADIAL RANGE: 4.40 TO 5.00 CM

ϕ ANGULAR RANGE

3.042 TO 3.142 RADIAN

0.000 TO 0.100 RADIAN

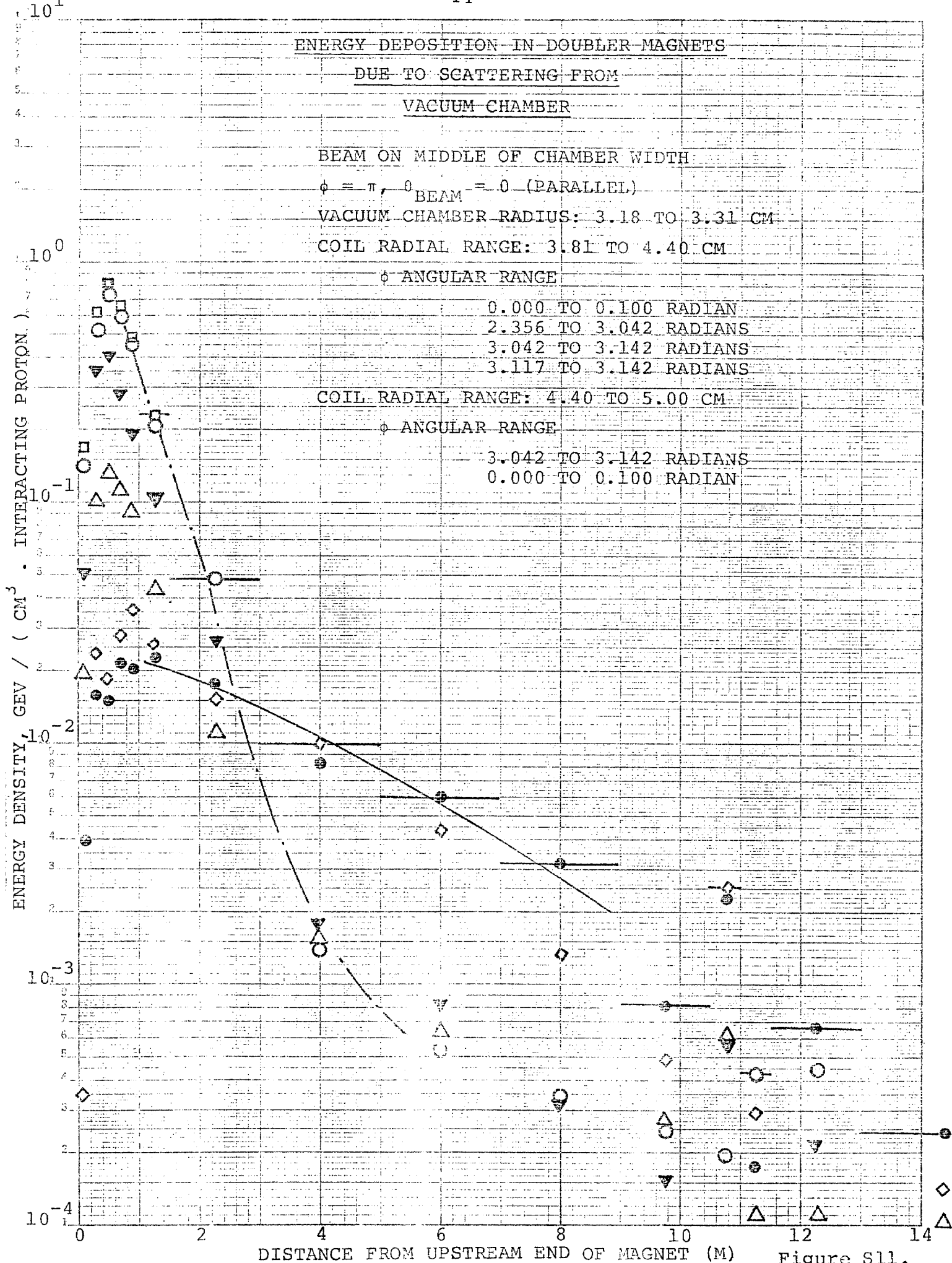


Figure S11.

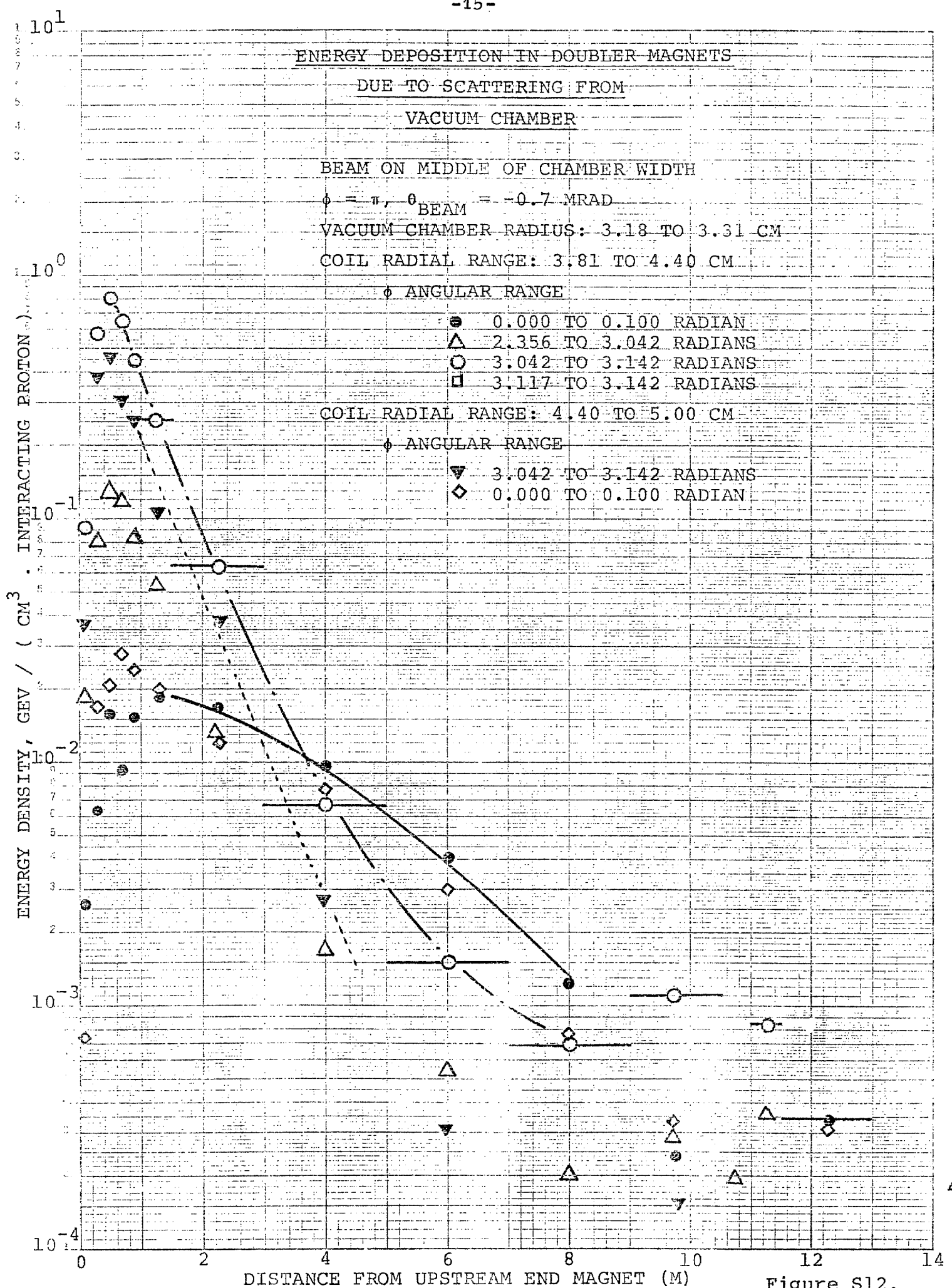


Figure S12.

ENERGY DEPOSITION IN DOUBLER MAGNETS
DUE TO SCATTERING FROM
VACUUM CHAMBER

BEAM ON OUTSIDE EDGE

$\phi = \pi, \theta = 0$ (PARALLEL)

VACUUM CHAMBER RADIUS: 3.18 TO 3.31 CM

COIL RADIAL RANGE: 3.81 TO 4.40 CM

ϕ ANGULAR RANGE

- 0.000 TO 0.100 RADIANS
- △ 2.356 TO 3.042 RADIANS
- 3.042 TO 3.142 RADIANS
- 3.117 TO 3.142 RADIANS

COIL RADIAL RANGE: 4.40 TO 5.00 CM

ϕ ANGULAR RANGE

- ▽ 3.042 TO 3.142 RADIANS
- ◇ 0.000 TO 0.100 RADIANS

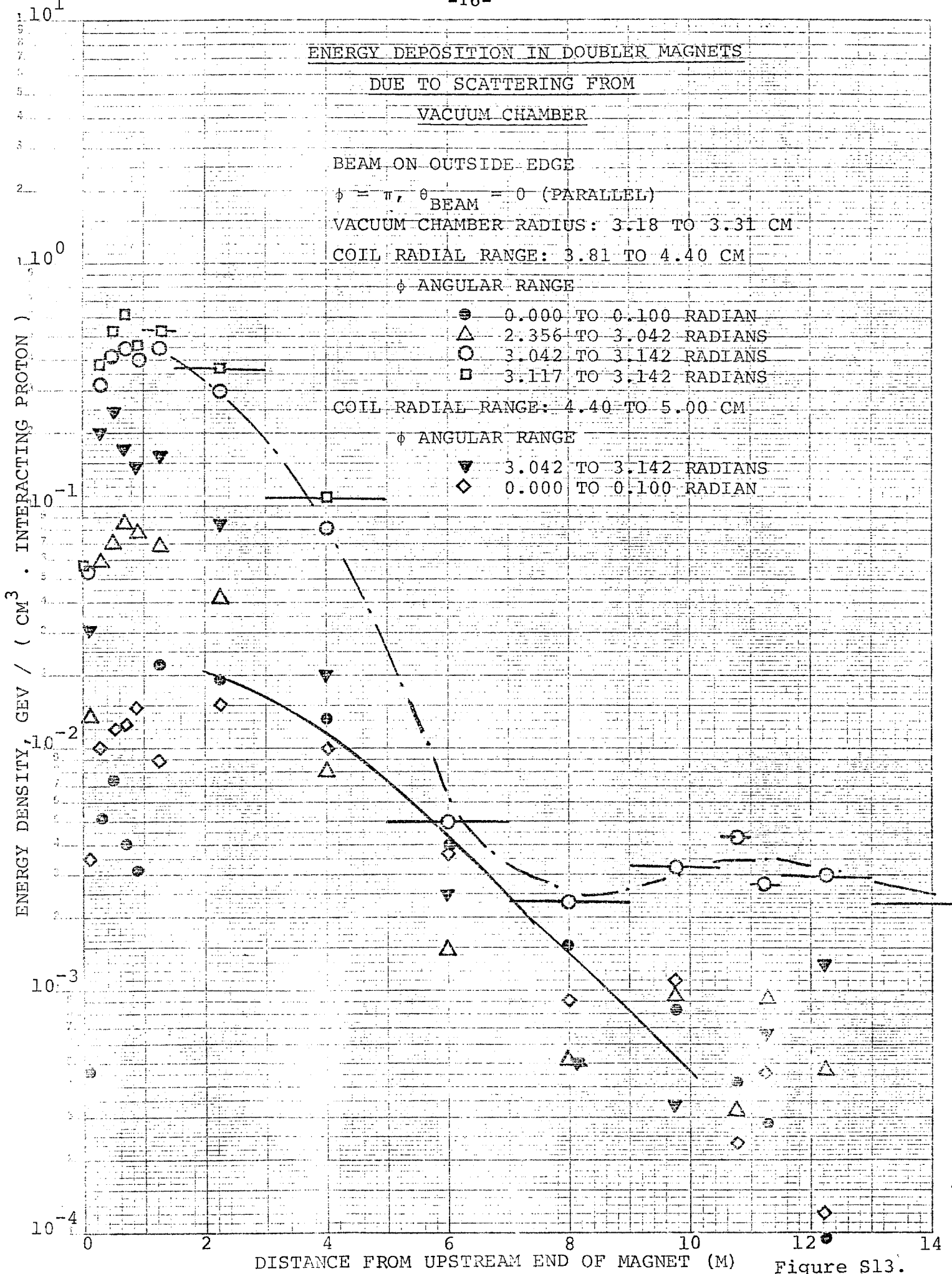


Figure S13.

ENERGY DEPOSITION IN DOUBLER MAGNETS

DUE TO SCATTERING FROM

VACUUM CHAMBER

BEAM ON INSIDE EDGE, $\theta = \pi$, $\theta_{\text{BEAM}} = 0$ (PARALLEL)

VACUUM CHAMBER RADIUS: 3.68 TO 3.81 CM

COIL RADIUS RANGE: 3.81 TO 4.40 CM

ϕ ANGLE RANGE

● 0.000 TO 0.100 RADIAN

△ 2.356 TO 3.042 RADIAN

○ 3.042 TO 3.142 RADIAN

□ 3.117 TO 3.142 RADIAN

COIL RADIUS RANGE: 4.40 TO 5.00 CM

ϕ ANGLE RANGE

▼ 3.042 TO 3.142 RADIAN

◇ 0.000 TO 0.100 RADIAN

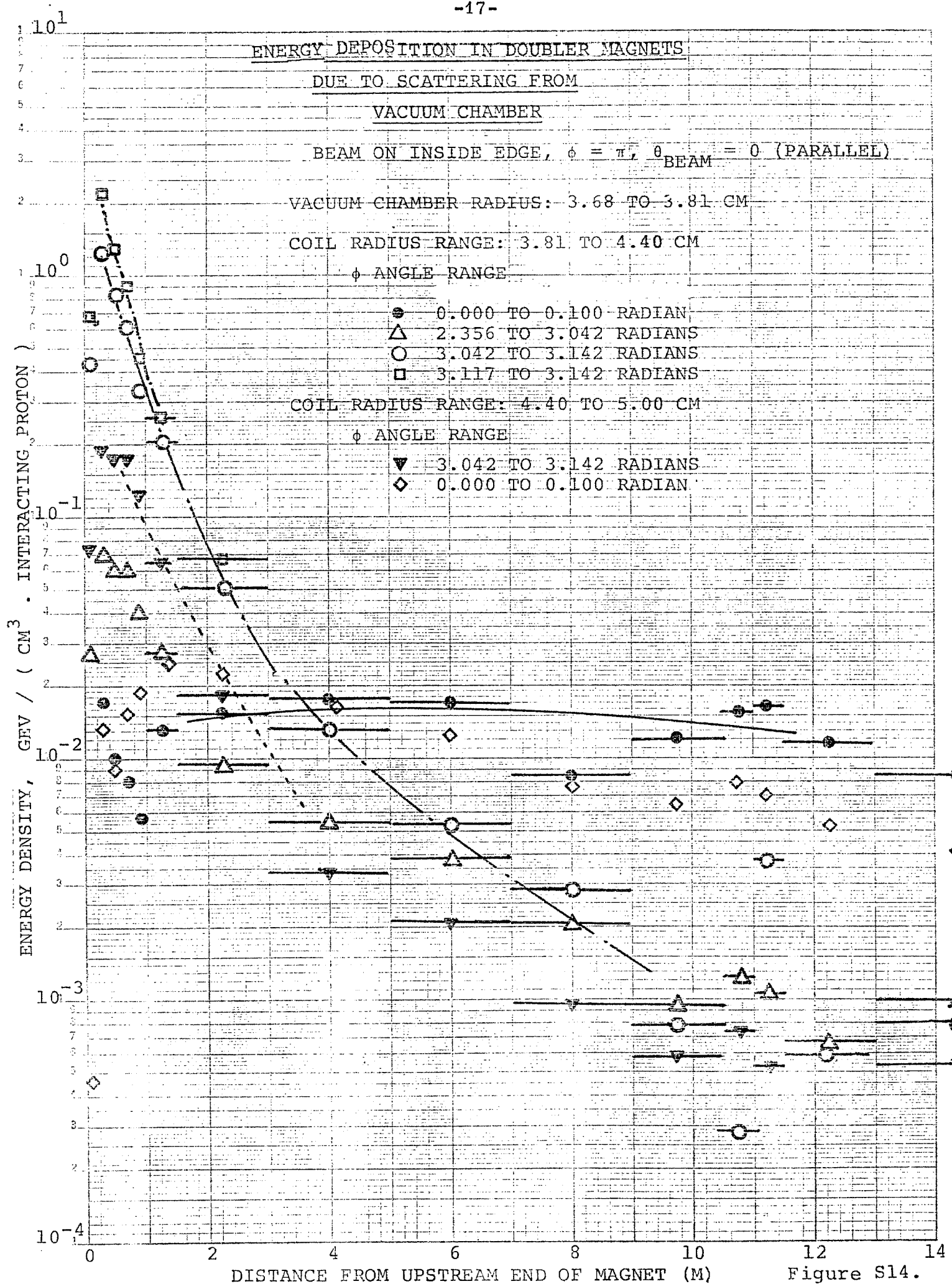


Figure S14.

ENERGY DEPOSITION IN DOUBLER MAGNETS
DUE TO SCATTERING FROM
VACUUM CHAMBER

BEAM ON INSIDE EDGE

$\phi = \pi$, $\theta_{\text{BEAM}} = -0.7$ MRAD

VACUUM CHAMBER RADIUS: 3.68 TO 3.81 CM

COIL RADIAL RANGE: 3.81 TO 4.40 CM

ϕ ANGULAR RANGE

● 0.000 TO 0.100 RADIANS

△ 2.356 TO 3.042 RADIANS

○ 3.042 TO 3.142 RADIANS

□ 3.117 TO 3.142 RADIANS

COIL RADIAL RANGE: 4.40 TO 5.00 CM

ϕ ANGULAR RANGE

▼ 3.042 TO 3.142 RADIANS

◇ 0.000 TO 0.100 RADIANS

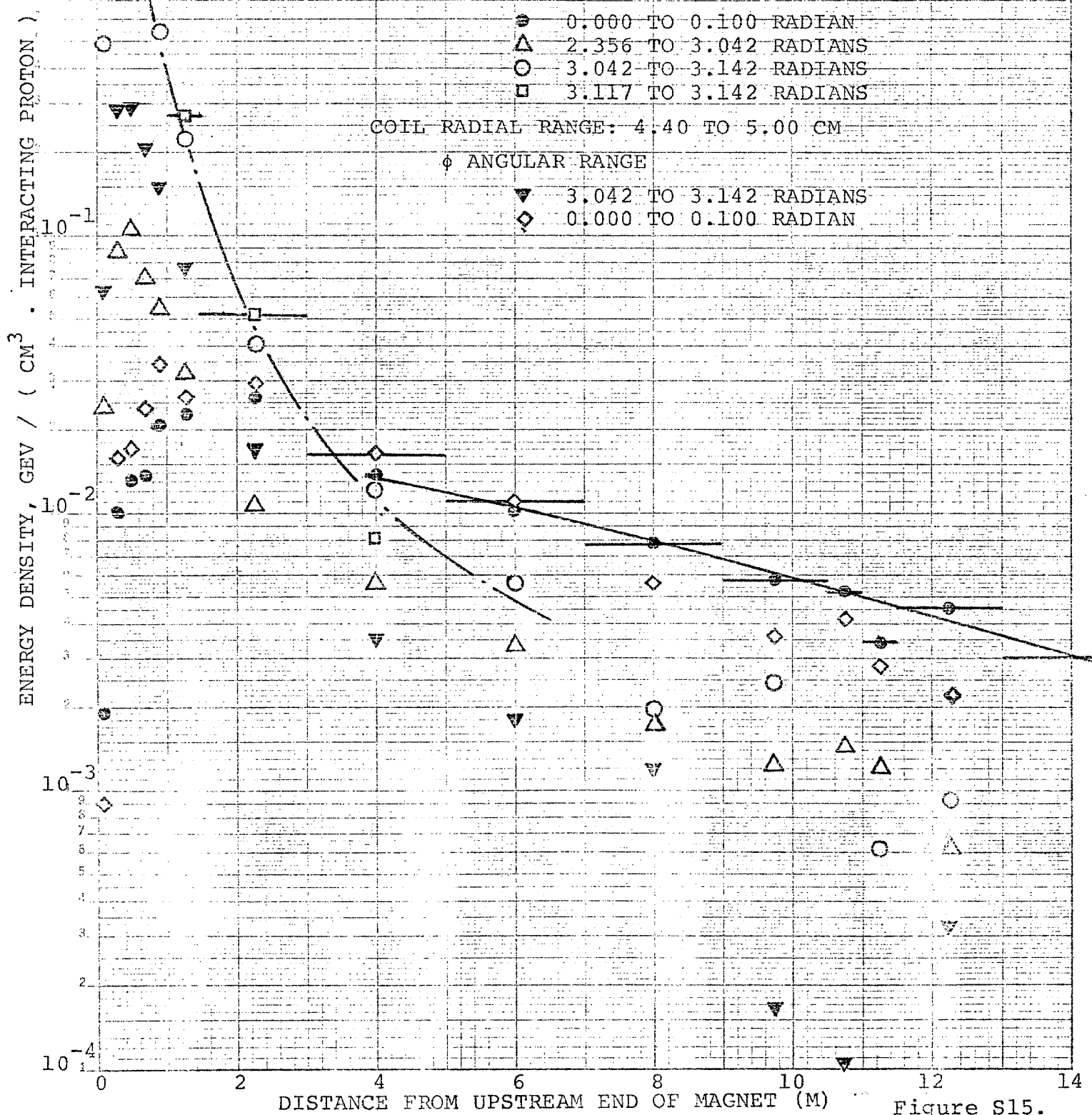


Figure S15.

ENERGY DEPOSITION IN DOUBLER MAGNETS

DUE TO SCATTERING FROM

VACUUM CHAMBER

BEAM ON MIDDLE OM CHAMBER WIDTH

$\phi = \pi/2$ BEAM = -0.7 MRAD

VACUUM CHAMBER RADIUS: 3.68 TO 3.81 CM

COIL RADIAL RANGE: 3.81 TO 4.40 CM

ϕ ANGULAR RANGE

● 0.000 TO 0.100 RADIAN

△ 2.356 TO 3.042 RADIAN

○ 3.042 TO 3.142 RADIAN

□ 3.117 TO 3.142 RADIAN

COIL RADIAL RANGE: 4.40 TO 5.00 CM

ϕ ANGULAR RANGE

▼ 3.042 TO 3.142 RADIAN

◇ 0.000 TO 0.100 RADIAN

ENERGY DENSITY, GEV / (CM³ · INTERACTING PROTON)

10¹

5

2

10⁰

10⁻¹

10⁻²

10⁻³

10⁻⁴

0

DISTANCE FROM UPSTREAM OF MAGNET (M)

Figure S16.

ENERGY DEPOSITION IN DOUBLER MAGNETS

DUE TO SCATTERING FROM

VACUUM CHAMBER

BEAM ON OUTSIDE EDGE

$\phi = \pi$, $\theta_{\text{BEAM}} = 0.7 \text{ MRAD}$

VACUUM CHAMBER RADIUS: 3.68 TO 3.81 CM

COIL RADIAL RANGE: 3.81 TO 4.40 CM

ϕ ANGULAR RANGE

● 0.000 TO 0.100 RADIANS

△ 2.356 TO 3.042 RADIANS

○ 3.042 TO 3.142 RADIANS

□ 3.117 TO 3.142 RADIANS

COIL RADIAL RANGE: 4.40 TO 5.00 CM

ϕ ANGULAR RANGE

▽ 3.042 TO 3.142 RADIANS

◇ 0.000 TO 0.100 RADIANS

10¹

10⁰

10⁻¹

10⁻²

10⁻³

10⁻⁴

10⁻⁵

10⁻⁶

10⁻⁷

10⁻⁸

10⁻⁹

10⁻¹⁰

10⁻¹¹

INTERACTING PROTON)

) CM³

) GEV

0 2 4 6 8 10 12 14

DISTANCE FROM UPSTREAM END OF MAGNET (M)

Figure S17.

ENERGY DEPOSITION IN DOUBLER MAGNETS

DUE TO SCATTERING FROM

VACUUM CHAMBER PLUG

PLUG: 5 CM. (H) X 3 CM. (V) APERTURE

BEAM ON INSIDE EDGE, $\phi = 0$, $\theta = 0$ BEAM

COIL RADIAL RANGE: 3.81 TO 4.40 CM

ϕ ANGULAR RANGE

□ 0.000 TO 0.025 RADIANS

● 0.000 TO 0.100 RADIANS

△ 0.100 TO 0.785 RADIANS

○ 3.042 TO 3.142 RADIANS

COIL RADIAL RANGE: 4.40 TO 5.00 CM

ϕ ANGULAR RANGE

▼ 0.000 TO 0.100 RADIANS

◇ 3.042 TO 3.142 RADIANS

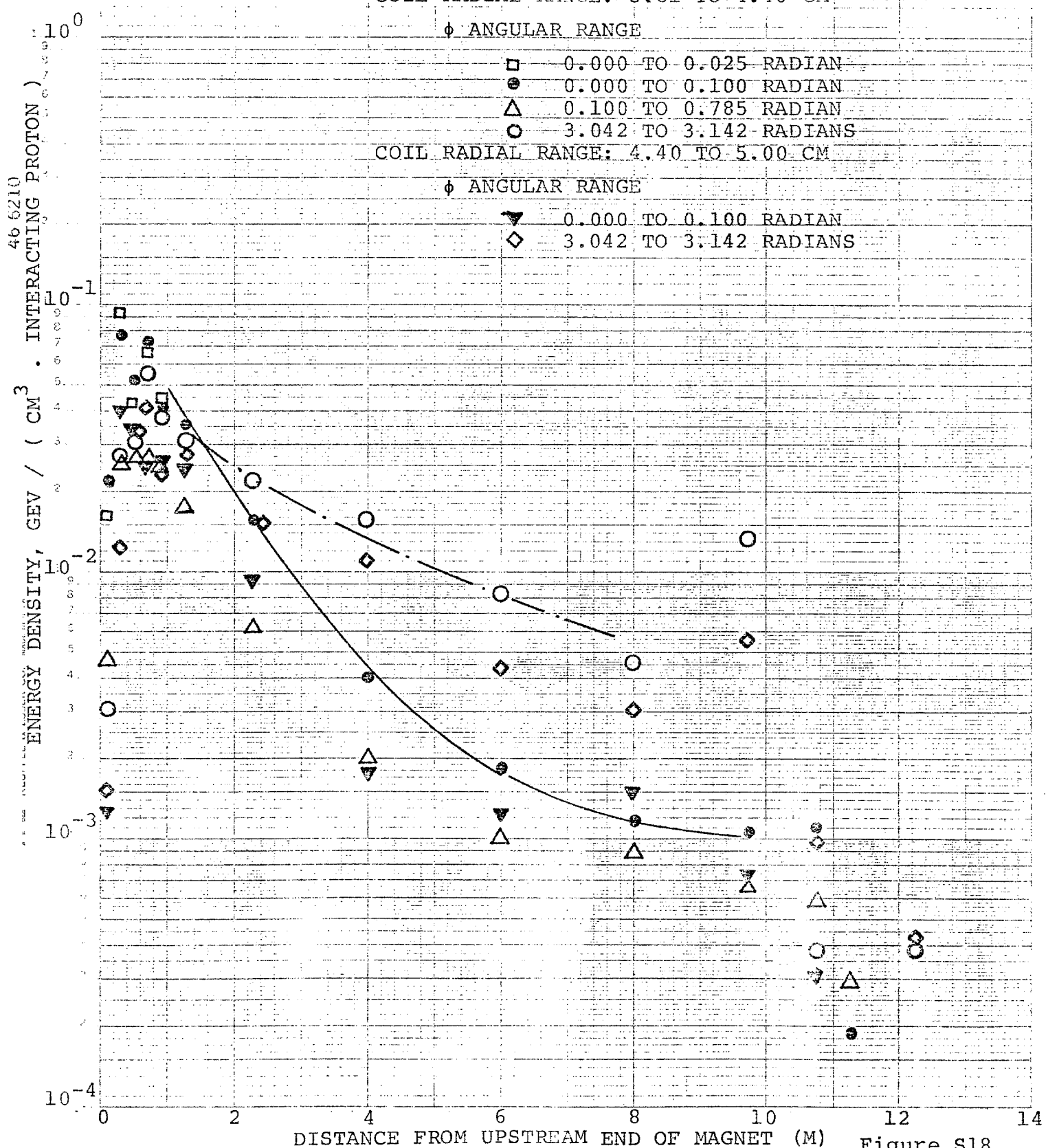


Figure S18.

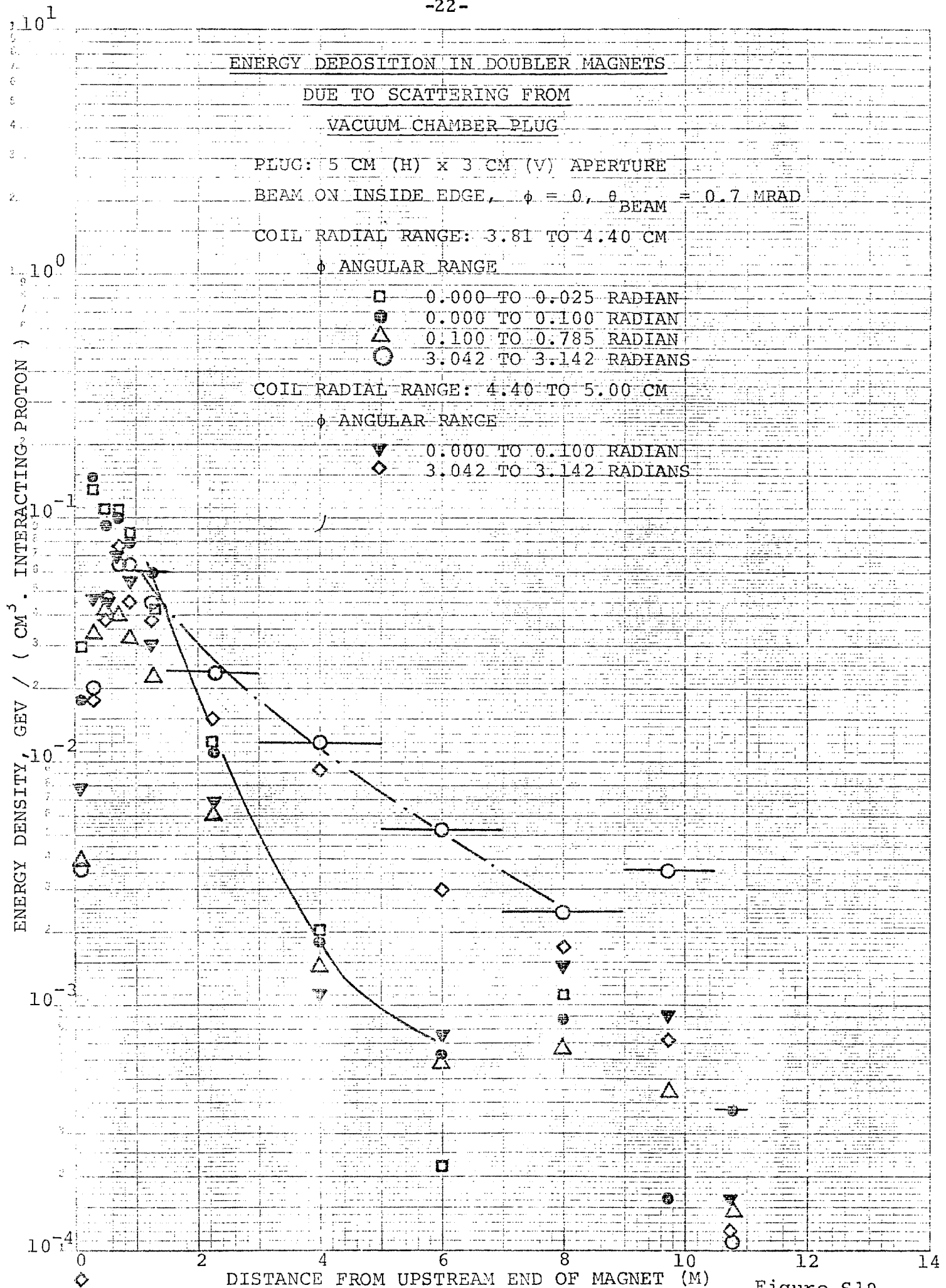


Figure S19.

ENERGY DEPOSITION IN DOUBLER MAGNETS

DUE TO SCATTERING FROM
VACUUM CHAMBER PLUG

PLUG: 5 CM (H) \times 3 CM (V) APERTURE

BEAM ON INSIDE EDGE, $\phi = \pi$, $\theta_{BEAM} = 0$

COIL RADIAL RANGE: 3.81 TO 4.40 CM

ϕ ANGULAR RANGE

● 0.000 TO 0.100 RADIANS

△ 2.356 TO 3.042 RADIANS

○ 3.042 TO 3.142 RADIANS

□ 3.117 TO 3.142 RADIANS

COIL RADIAL RANGE: 4.40 TO 5.00 CM

ϕ ANGULAR RANGE

▼ 3.042 TO 3.142 RADIANS

◇ 0.000 TO 0.100 RADIANS

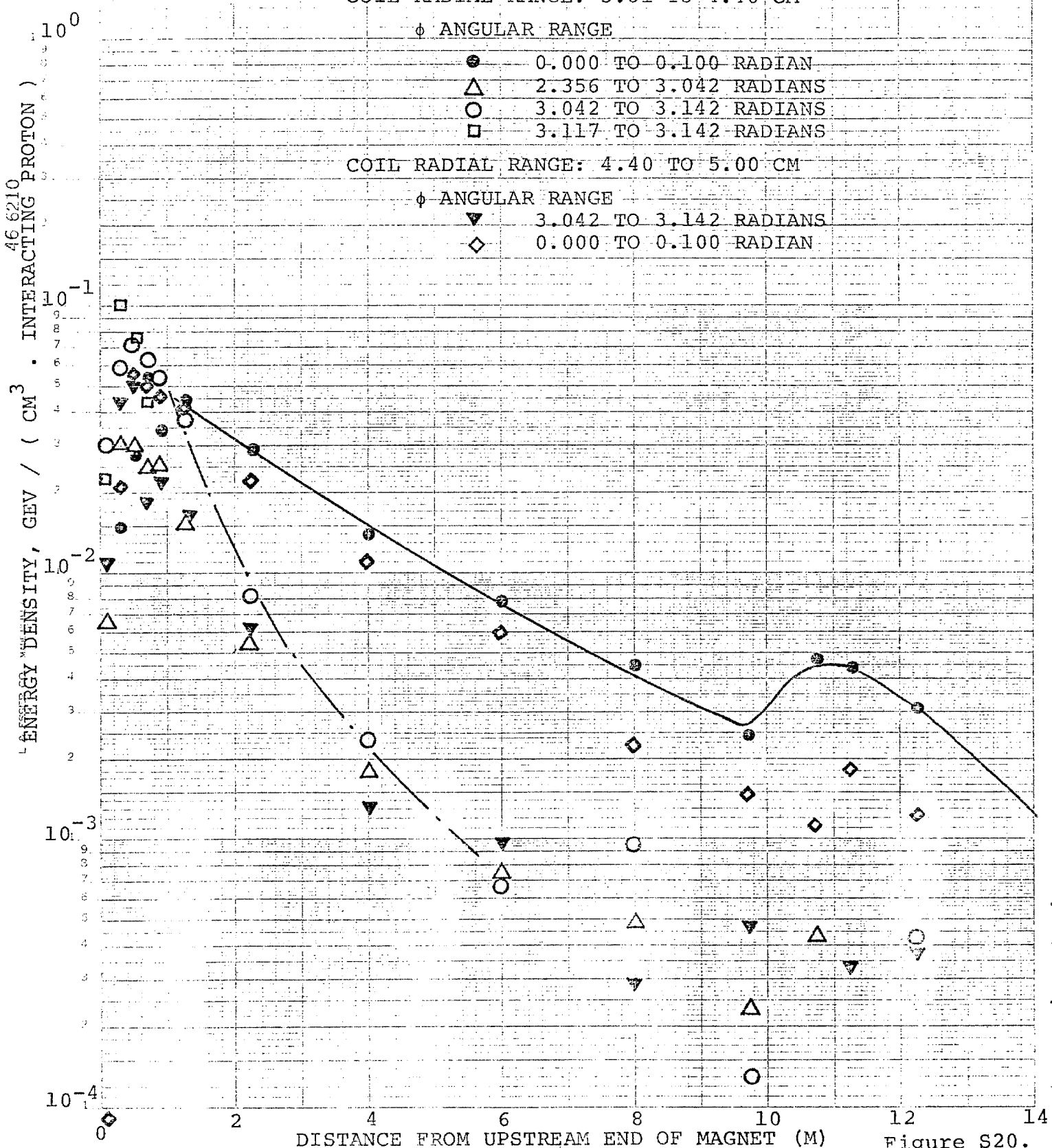


Figure S20.

ENERGY DEPOSITION IN DOUBLER MAGNETS
DUE TO SCATTERING FROM
VACUUM CHAMBER PLUG

PLUG: 5 CM (H) X 3 CM (V) APERTURE

BEAM ON INSIDE EDGE, $\phi = \pi$, $\theta_{\text{BEAM}} = -0.7 \text{ MRAD}$

COIL RADIAL RANGE: 3.81 TO 4.40 CM

ϕ ANGULAR RANGE

● 0.000 TO 0.100 RADIANS

△ 2.356 TO 3.042 RADIANS

○ 3.042 TO 3.142 RADIANS

□ 3.117 TO 3.142 RADIANS

COIL RADIAL RANGE: 4.40 TO 5.00 CM

ϕ ANGULAR RANGE

▽ 3.042 TO 3.142 RADIANS

◇ 0.000 TO 0.100 RADIANS

ENERGY DENSITY, GEV / (CM³ . INTERACTING PROTON)

10¹

10⁰

10⁻¹

10⁻²

10⁻³

10⁻⁴

DISTANCE FROM UPSTREAM END OF MAGNET (M)

0

2

6

8

10

12

14

Figure S21.

SUPPLEMENT TO UPC 40

Figures S22 through S25 show energy density distributions in the Doubler magnet coils due to scattering from a beam scraper at a medium straight section. The iron beam scraper with an aperture of 4.5 cm(horizontal) by 2 cm(vertical) and 2 m in length is placed 12 m upstream of the Doubler magnets. The incident proton energy is 1000 GeV. The beam strikes an inside edge of the scraper with an incident angle of 0 mrad. The ϕ angle is π in Figures S22, S23, and S24 and 0 in Figure S25. In Figure S22 beam collimator and vacuum chamber plug are not present. The vacuum chamber radius is 3.68 to 3.81 cm. The vacuum chamber plug with a 5 cm(H) by 3 cm(V) aperture is added in Figure S23. In Figures S24 and S25 a 2 m long iron collimator with a 5 cm(H) by 3 cm(V) aperture is placed immediately upstream of the Doubler magnets. The plug and collimator reduce the peak energy density to about 6×10^{-3} GeV/(cm³.interacting proton) from 4×10^{-2} GeV/(cm³.interacting proton).

Figures S26 through S33 show energy density distributions due to scattering from the extraction wire septum for various configurations of the beam bump arrangement at the long straight section. Four B-2 type bending magnets are used for the beam bump of 3 mrad as shown in Figure 6. The incident proton energy is 1000 GeV. A string of four quadrupole magnets which are to be placed upstream of the dipole string are omitted in the present study. Figure S26 is essentially the same as Figure 3 in which beam bump, vacuum chamber plug and collimator are not present. A small discrepancy at the upstream end is due to different

binnings in the two cases.

Table II summarizes the conditions and peak energy densities.

Table II. Peak energy densities due to scattering from the extraction electrostatic wire septum for various configurations shown in Figures S26 through S33.

Figure	Plug	Beam Bump	Collimator	Peak Energy Density GeV/(cm ³ · incid. prot.)	
				First	Second
S26	No	No	No	4×10^{-3}	2×10^{-3}
S27	Yes	No	Yes	9×10^{-4}	6×10^{-4}
S28	No	4M, H-In	-	-	9×10^{-4}
S29	No	3M, H-In	-	-	4×10^{-4}
S30	Yes	3M, H-In	-	2×10^{-4}	5×10^{-5}
S31	Yes	3M, H-Out	-	2×10^{-4}	6×10^{-5}
S32	No	3M, V	-	-	8×10^{-5}
S33	Yes	3M, V	-	5×10^{-5}	4×10^{-5}

The 2 m long iron collimator with an aperture of 5 cm(H) by 3 cm(V) is used only in Figure S27. The vacuum chamber plug is made of iron and has an aperture of 5 cm(H) by 3 cm(V). The beam bumps, 4M and 3M correspond to the arrangements in which the electrostatic wire septum is placed upstream and downstream of the first bump magnet, respectively. The H-In and H-Out are the horizontal inward and outward bumps and the V is the vertical beam bump. The horizontal inward bump arrangement is slightly better than the horizontal outward bump when the vacuum chamber plug is not used, but

they are essentially the same when the plug is used. In general, the vertical bump gives much lower peak energy density in the Doubler magnet coils than the horizontal bump because the narrow vertical aperture of the bump magnets is more efficient to absorb off-momentum secondary particles scattered from septum wires.

The peak energy density of 5×10^{-5} GeV/(cm³.incident proton) achieved by the vertical bump (Figure S33) gives the limits for extraction due to scattering from the electrostatic wire septum of 4.5×10^{14} protons/sec for slow extraction and 1.2×10^{14} protons/pulse of 1 msec. The extraction inefficiency was assumed to be 2.5 %, i.e. 2.5 % of protons strike septum wires.

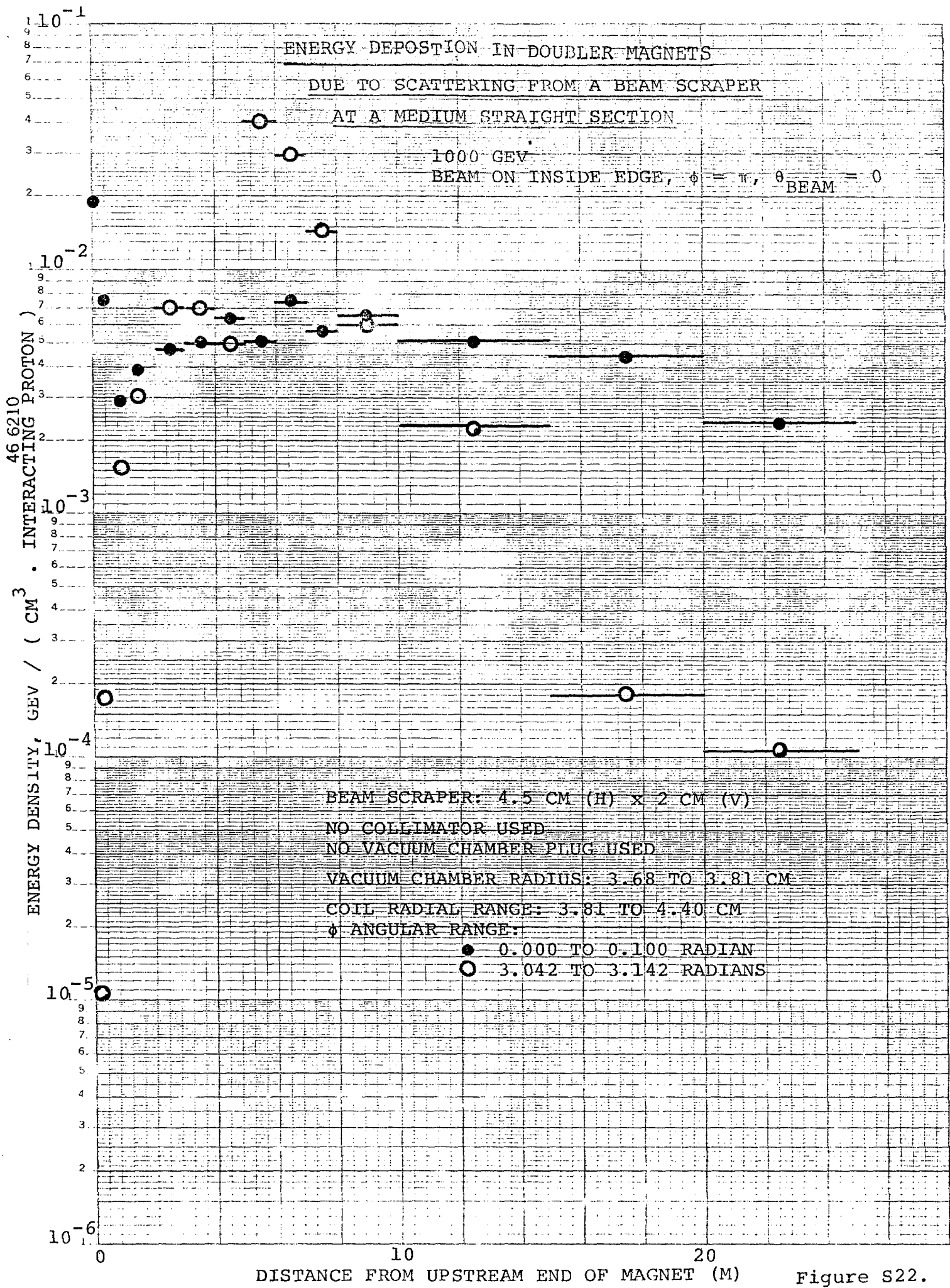


Figure S22.

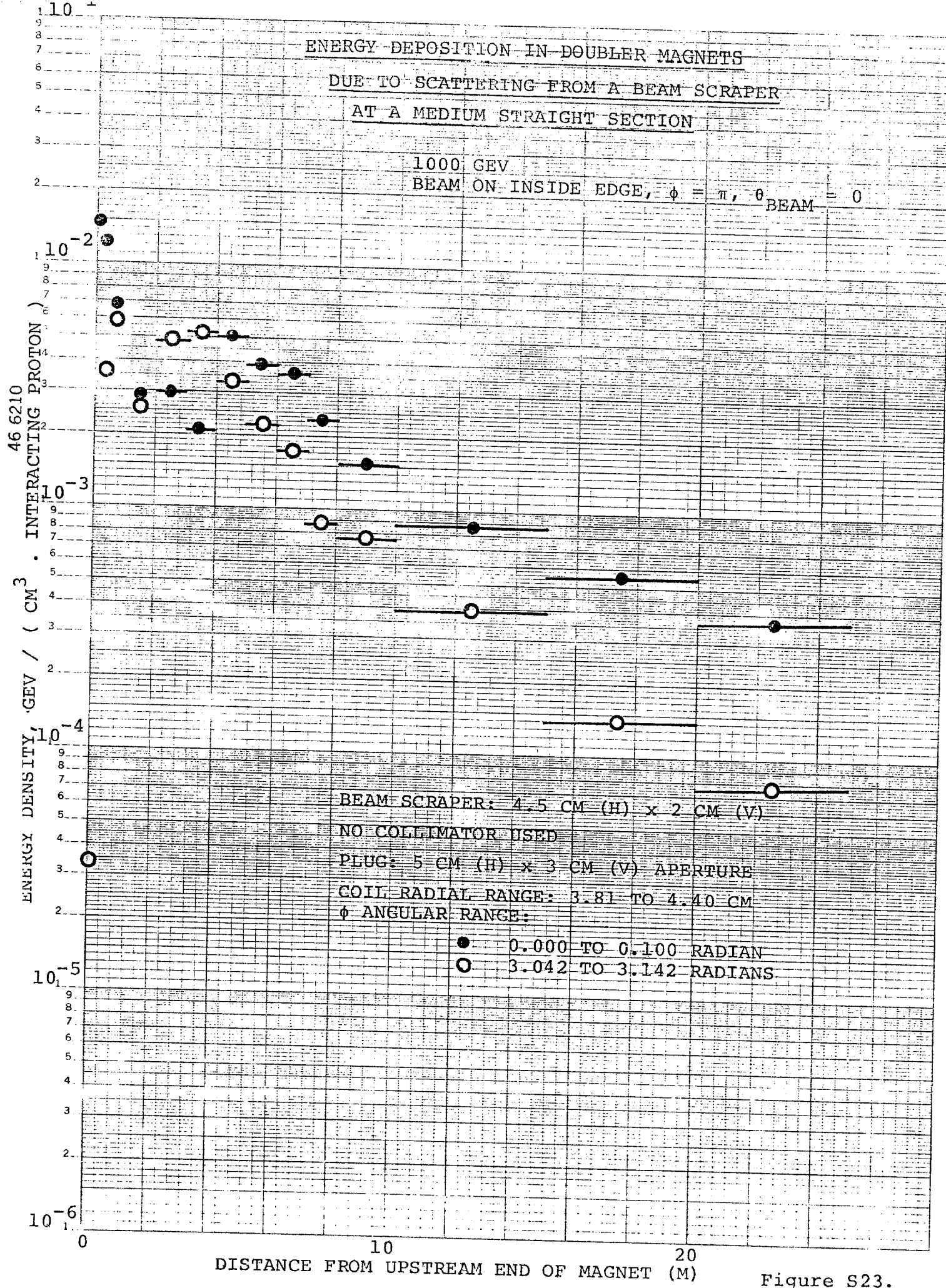


Figure S23.

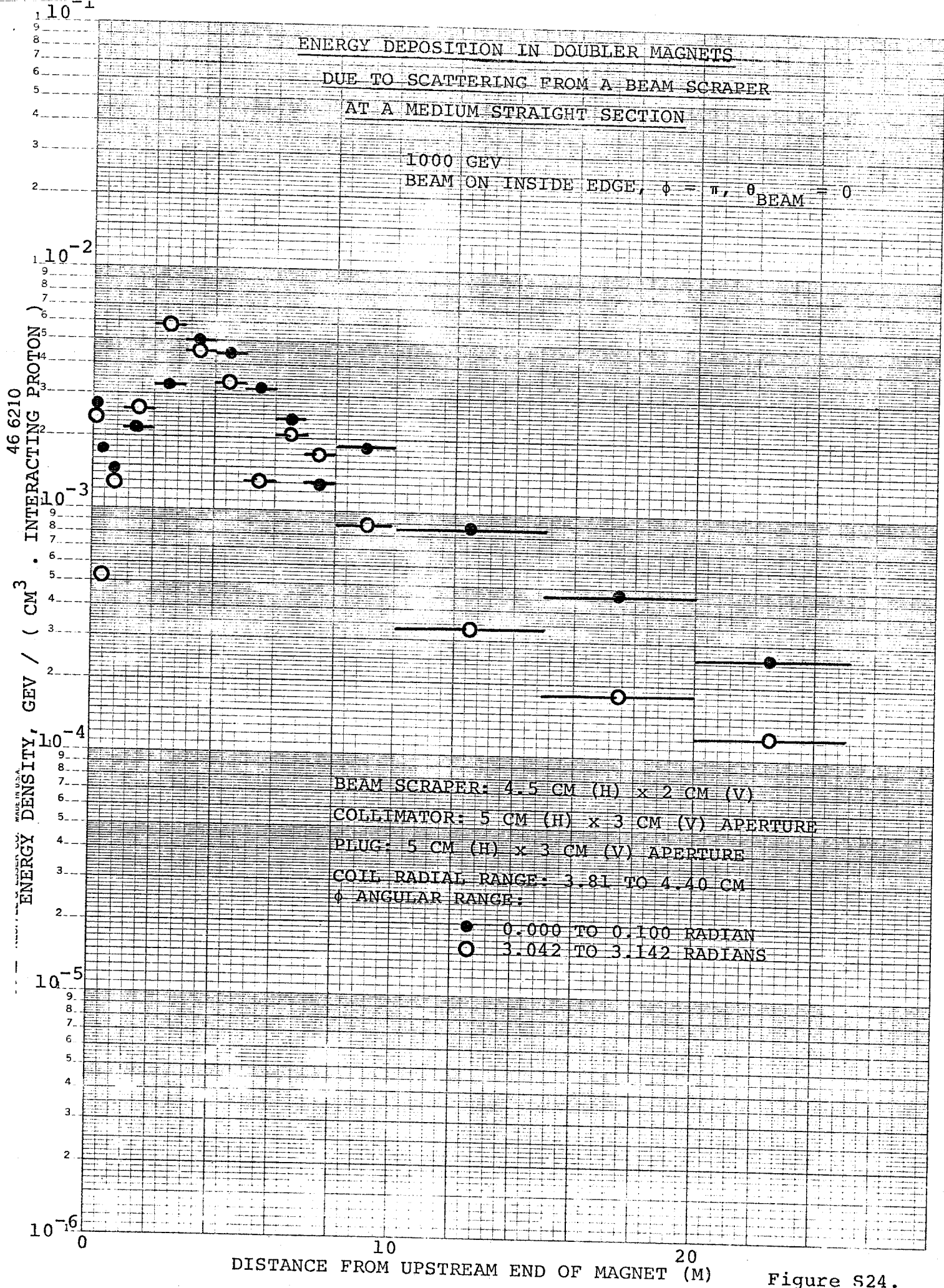


Figure S24.

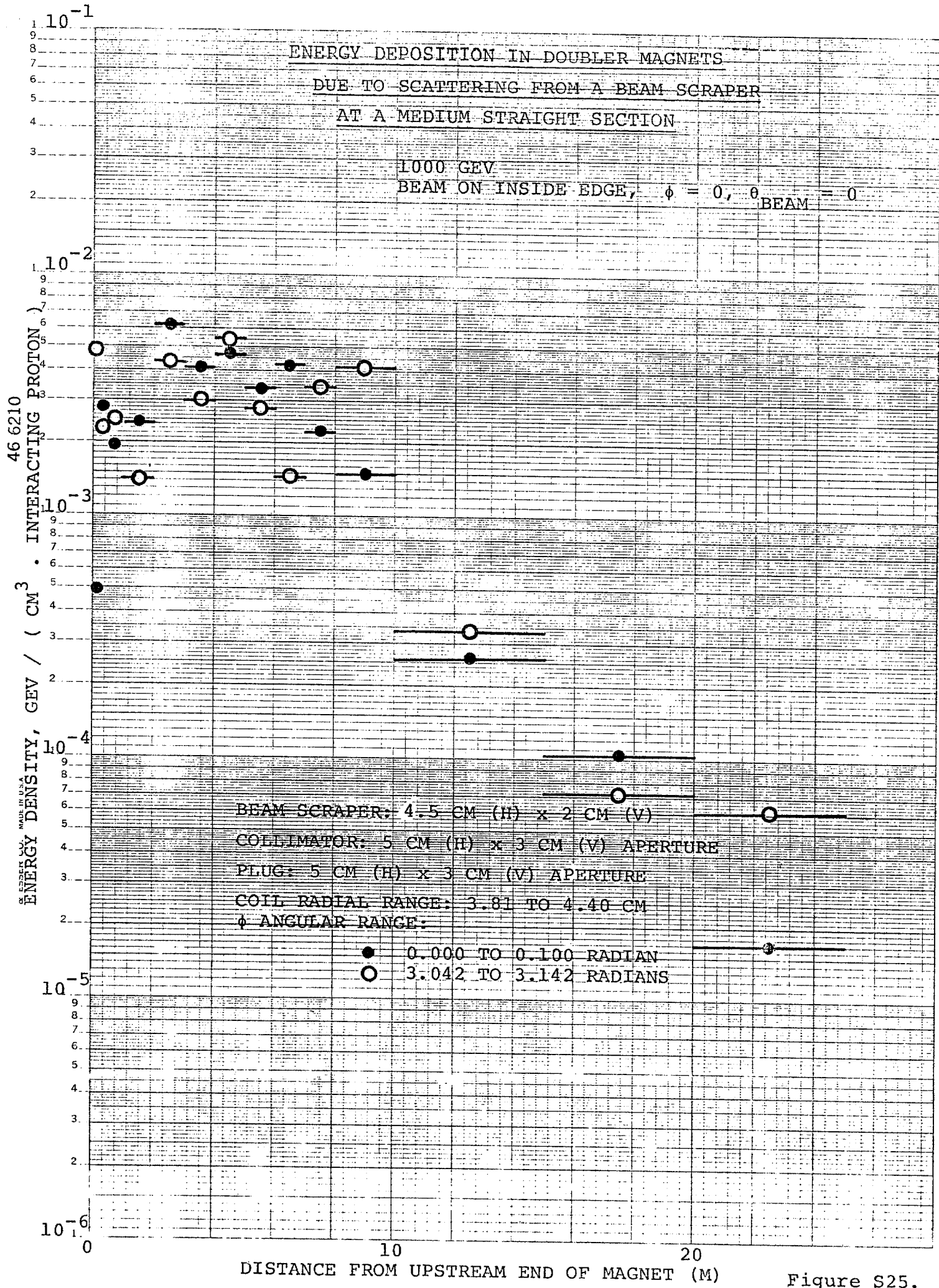


Figure S25.

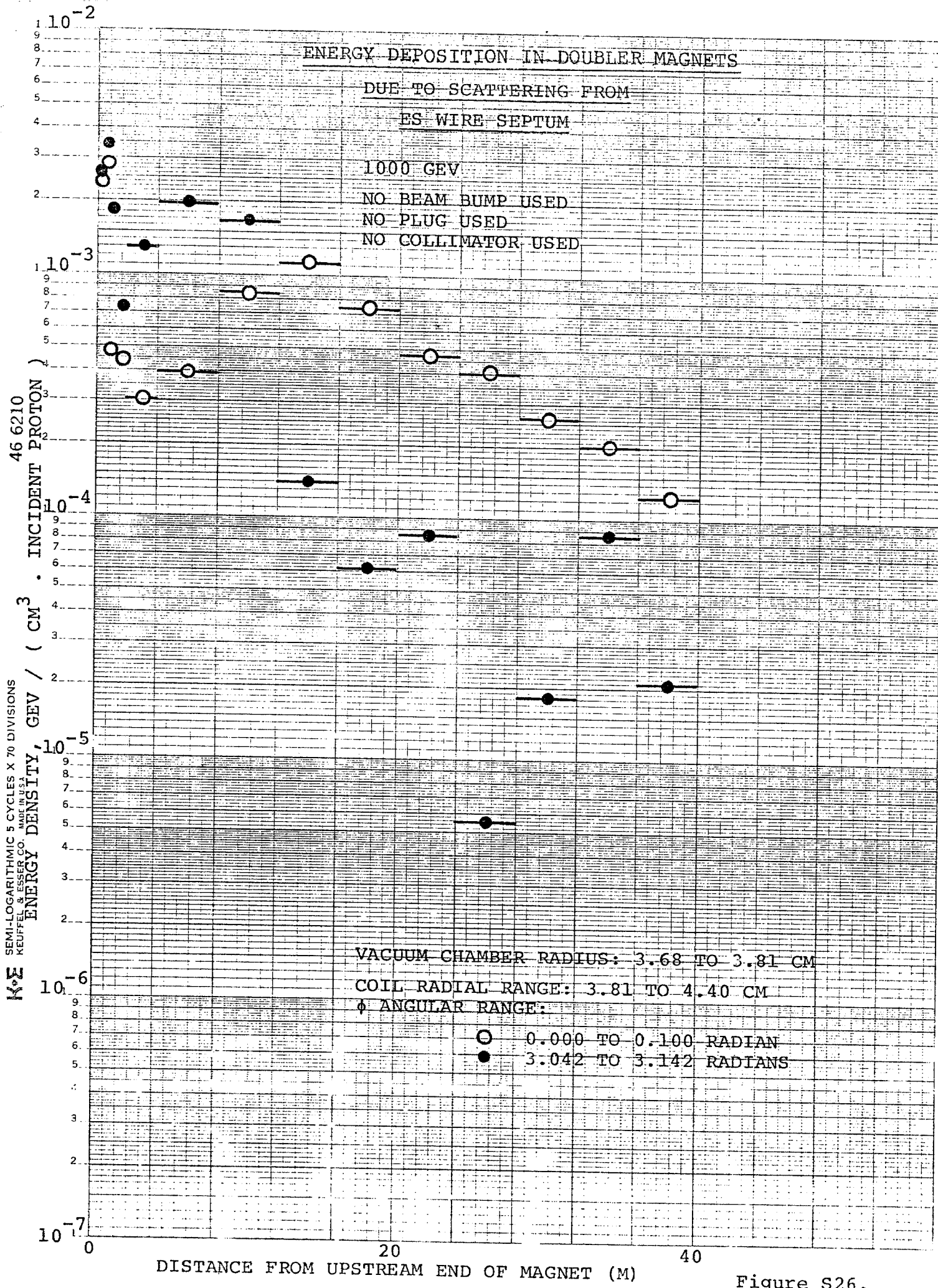


Figure S26.

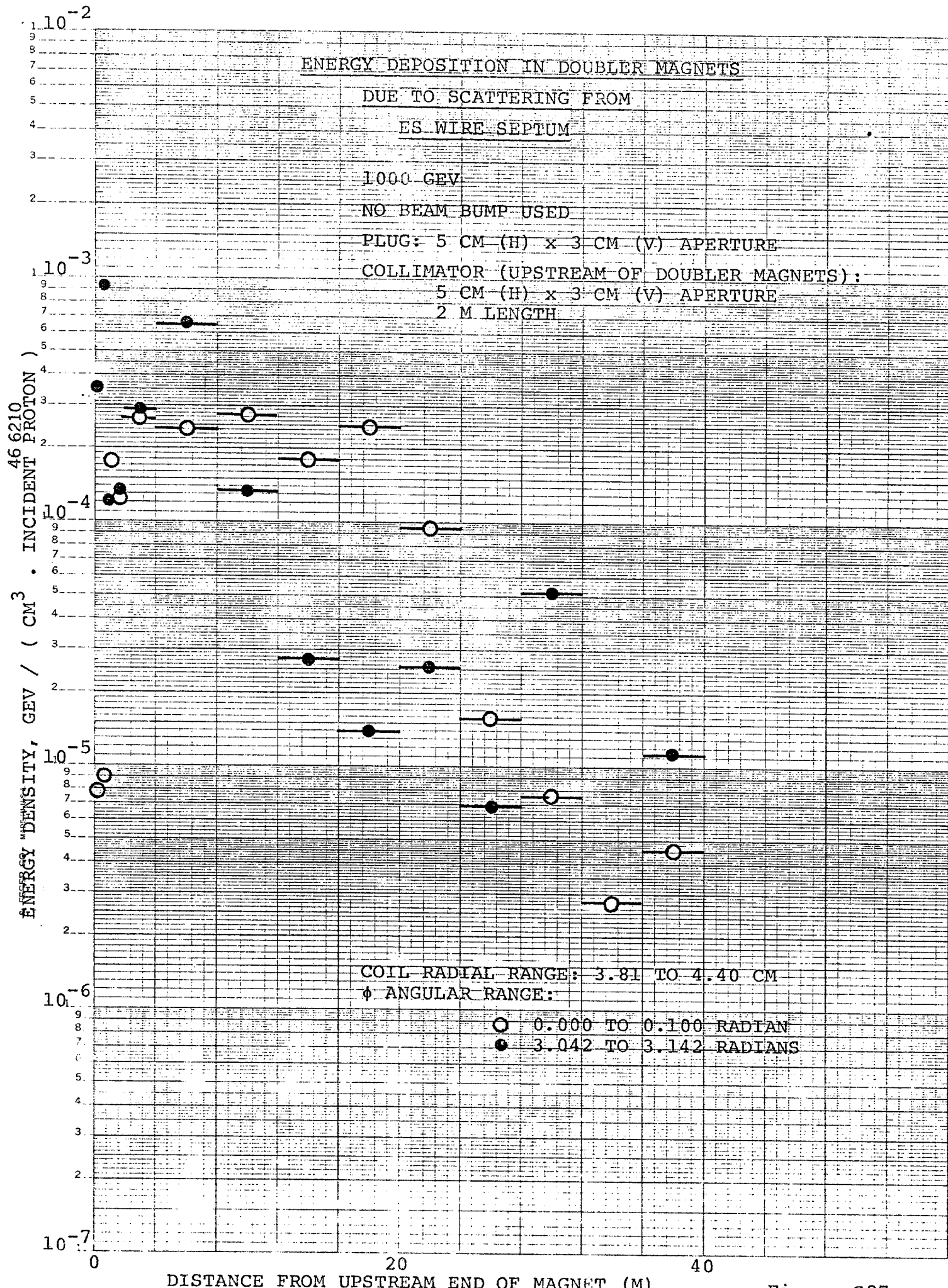


Figure S27.

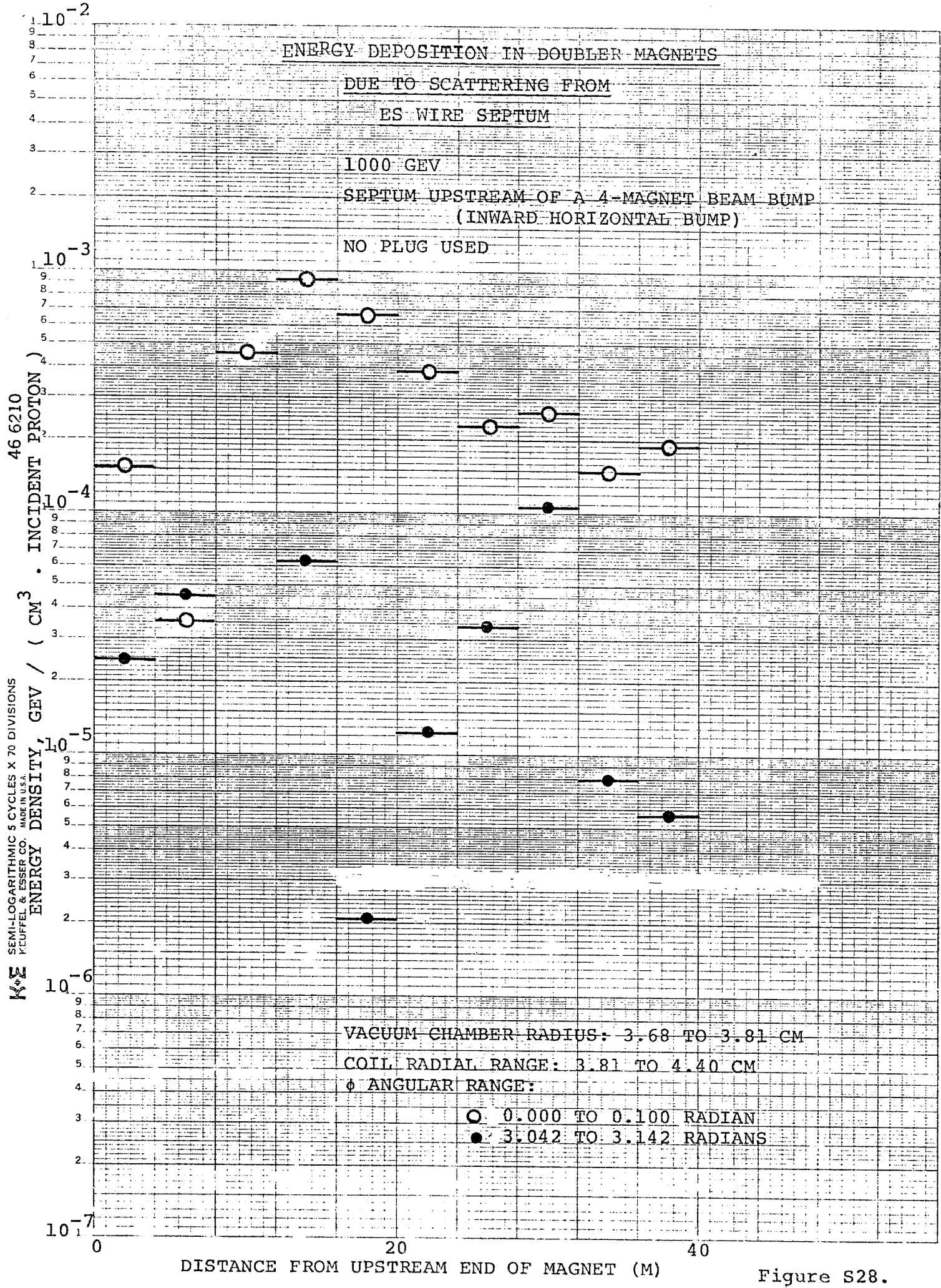


Figure S28.

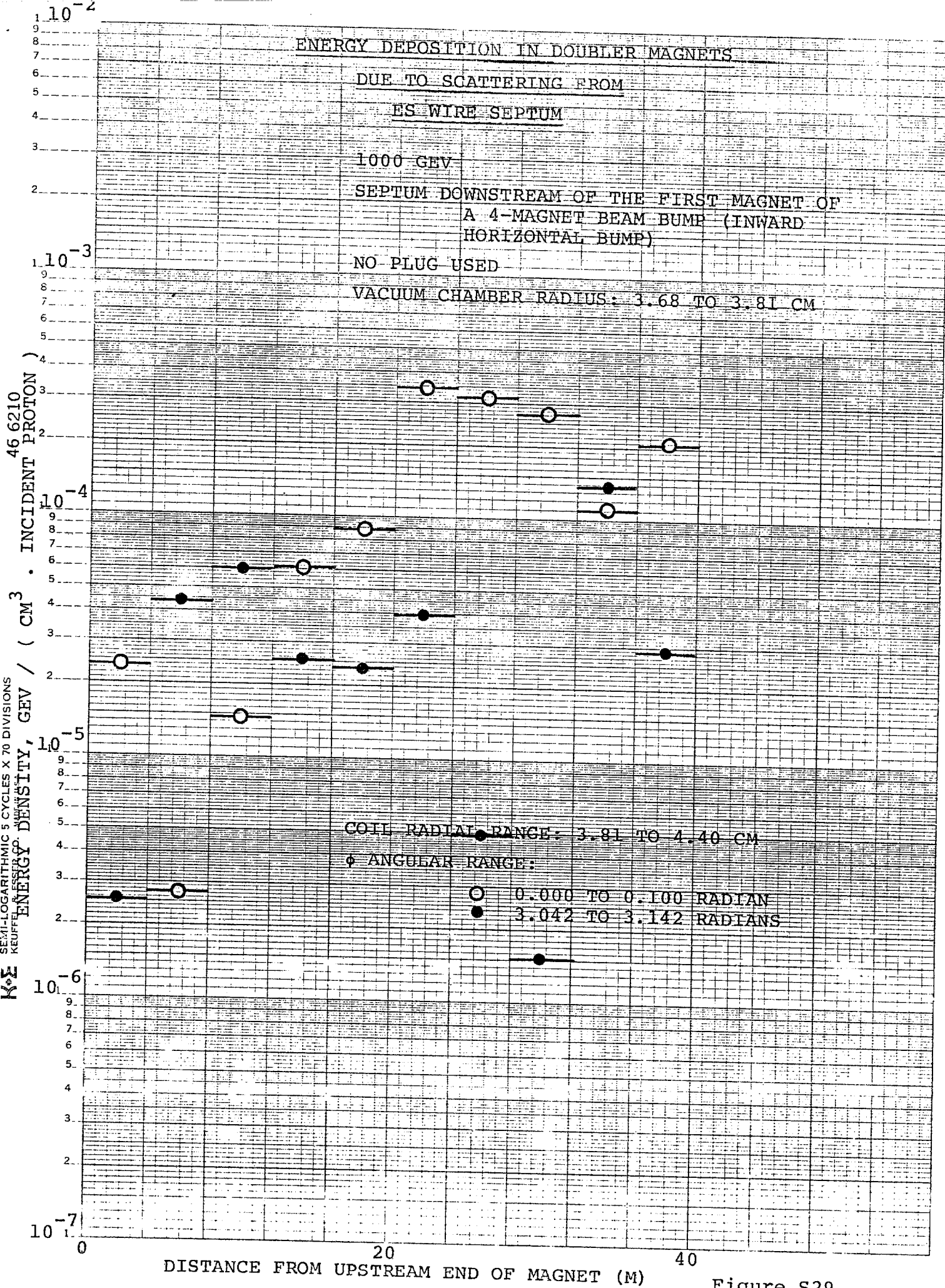


Figure S29.

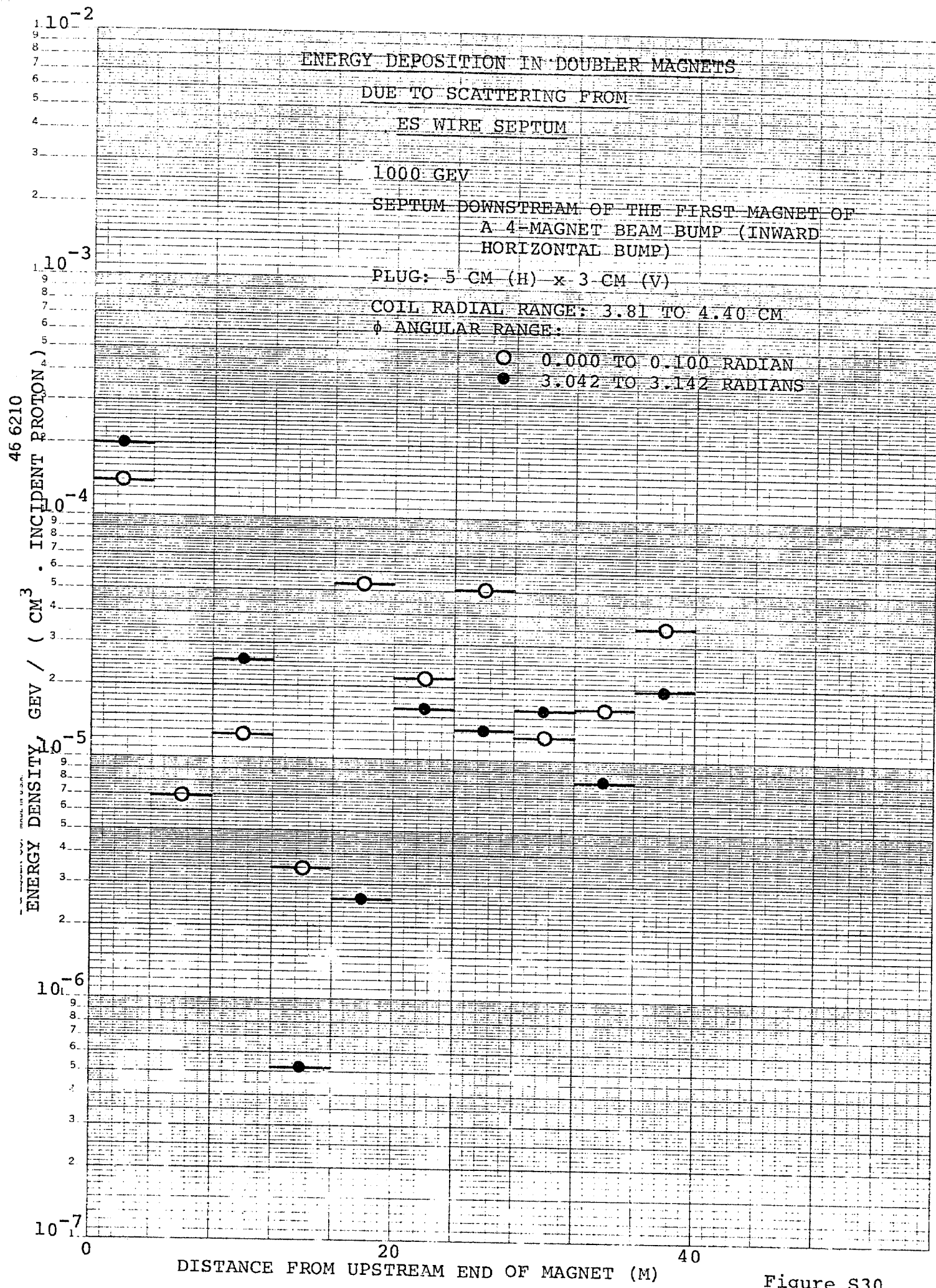
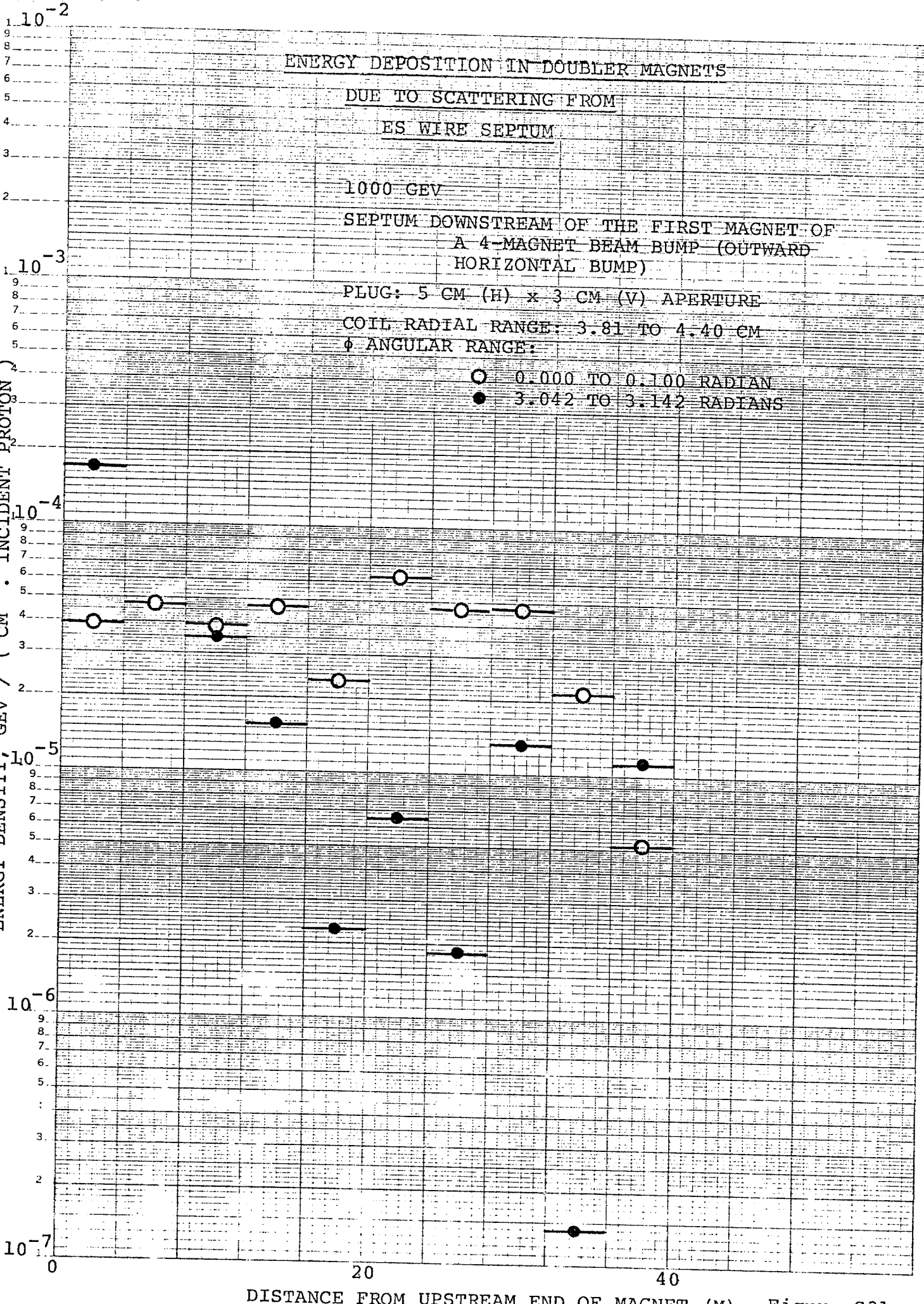


Figure S30.

KELFEL & ESSER CO. MADE IN U.S.A. SEMI-LOGARITHMIC 5 CYCLES X 70 DIVISIONS

46 6210
ENERGY DENSITY, GEV / (CM³ · INCIDENT PROTON)



DISTANCE FROM UPSTREAM END OF MAGNET (M)

Figure S31.

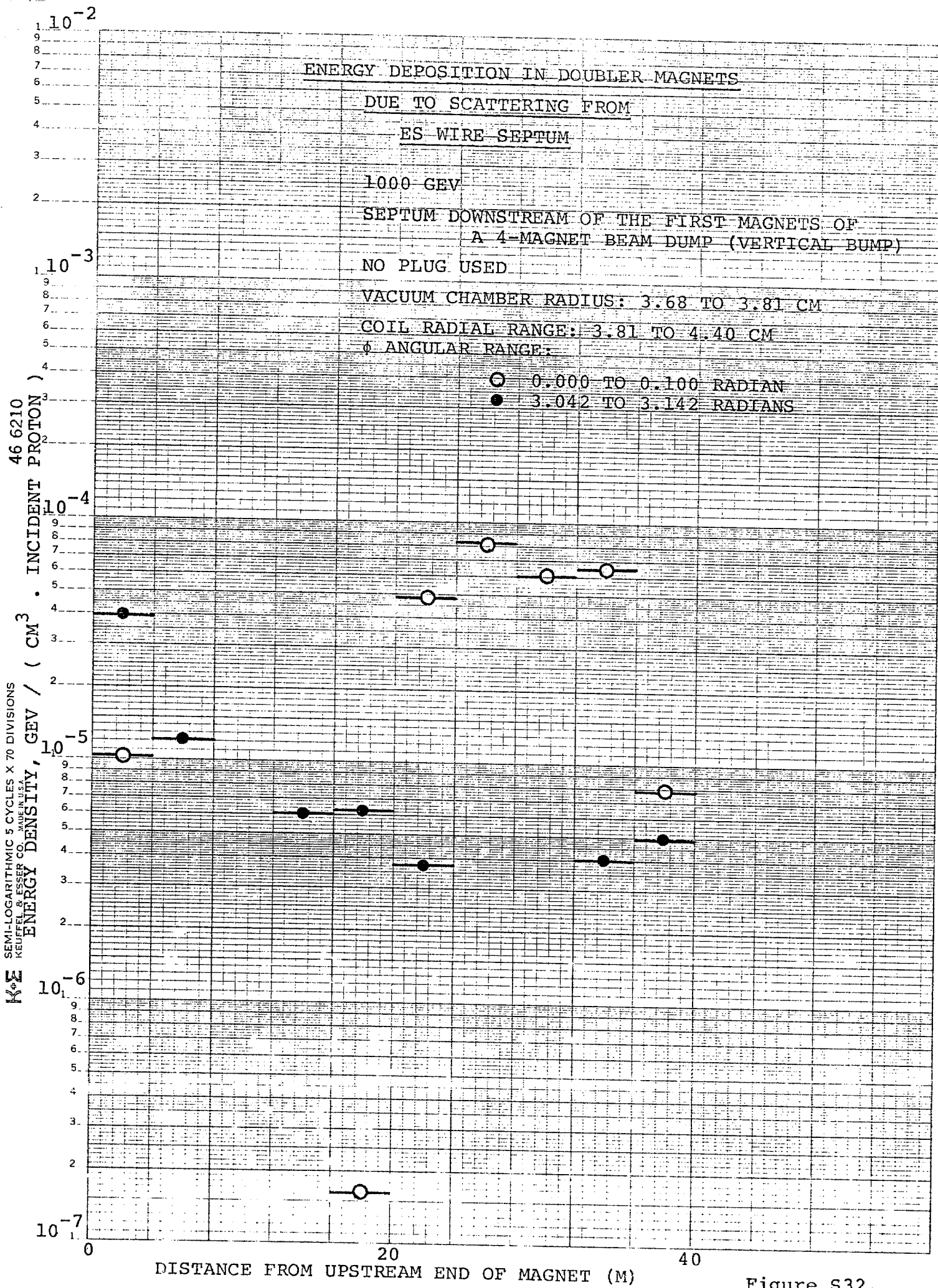


Figure S32.

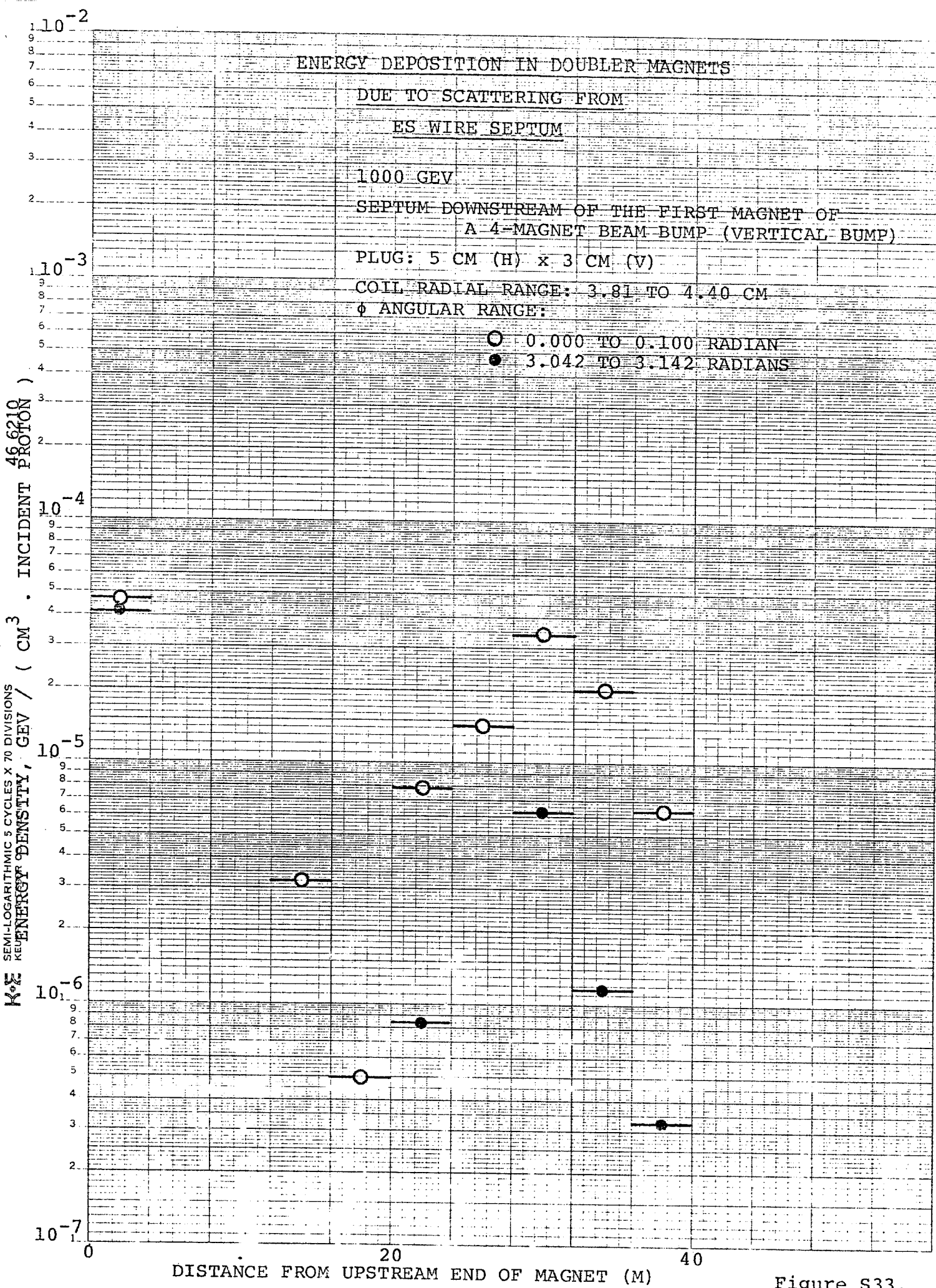


Figure S33.